FABRICATION OF PHOTONIC CRYSTAL AQUEOUS SULFATE ANIONS SENSING MATERIAL

by

Sylvere N. Sirikare

B.S Laroche College, 2003

Submitted to the Graduate Faculty of

Arts and Sciences in partial fulfillment

of the requirements for the degree of

Master in Chemistry

University of Pittsburgh

2006

UNIVERSITY OF PITTSBURGH

DEPARTEMENT OF CHEMISTRY

This thesis was presented

By Sylvere N. Sirikare

It was defended on

January /20 /2006

and approved by

Professor Christian E. Schafmeister, Department of Chemistry

Professor Adrian Michael, Department of Chemistry

Professor Sanford A. Asher, Advisor: Department of Chemistry

FABRICATION OF PHOTONIC CRYSTAL AQUEOUS SULFATE ANIONS SENSING MATERIAL

Sylvere N. Sirikare, M.S.

University of Pittsburgh, 2006

The focus of this thesis is the fabrication of an Intelligent Polymerized Crystalline Colloidal Array (IPCCA) photonic material that may sense sulfate anions using a charged amide-amine macrocyclic compound (PyEAmNH$_3^+$) in pure water at low concentrations. Sulfate (SO$_4^{2-}$) anions were found to bind to a charged amide-amine macrocyclic compound (PyEAmNH$_3^+$) in DMSO. (Dr Bowman-James and Dr Kang, University of Kansas). In this work, (PyEAmNH$_3^+$) is covalently attached to a PCCA to forms an intelligent polymerized crystalline colloidal array (IPCCA) which would sense SO$_4^{2-}$. However, we have demonstrated that our IPCCA did not bind to sulfate anions, rather the IPCCA response is due to the change in ionic strength and pH.

TABLE OF CONTENTS

LIST OF TABLES

LIST OF FIGURES

ACKNOWLEDGEMENTS

I would like to express gratitude to my research advisor, Professor Sanford A. Asher, for the support, encouragement, that he generously provided during my graduate studies at the University of Pittsburgh.

I would also like to thank Dr. Vladmir Alexeev, Dr Matti Ben-Moshe and Zeeshan Ahmed for their scientific insight and encouragement. They greatly contributed to my growth as a scientist. Also, I would like to thank all of the past and present members of the Asher research group for their support and friendship.

.   I gratefully acknowledge Professor Bowman-James and Dr Kang for synthesizing the ligand which made the work described in Chapter 2 possible. This work was financially supported by the NIH.

I would especially like to thank all the teachers and professors who have guided me along my educational career, especially Professor Kaburungu and Professor Roberta Hartman former undergraduate advisors .To them I owe my early success in Science .

I would like to express special thanks to my parents, Felicite and Edouard. To them I owe my thirst for knowledge and love of truth. Thank you for your love. My thanks go to my sister Brigitte, brother Naramabuye and Brother Rene for being the bridge of my opportunities.

Finally, I would like to thank my wife to be, Chantal, for her love, understanding and support over the past three years. I am looking forward to many more wonderful years together

1.0   INTRODUCTION TO PCCA SENSING MATERIALS

1.1   THE CRYSTALLINE COLLOIDAL ARRAY

This report describes an application of novel optical materials that contain mesoscopically periodic arrays of polystyrene colloidal particles, called Crystalline Colloidal Arrays (CCAs). [1-3] The CCAs diffract visible light according to Bragg's law, and the wavelength of diffraction depends upon the interparticle spacing. These materials can be used to make a thin diffracting film and have applications as tunable filters, sensors, and optical switches. [4-9]

Crystalline colloidal arrays are three-dimensional periodic structures (**Figure 1**), which self-assemble from suspensions of highly charged, monodisperse colloidal particles in low ionic strength solution. The surface charge on the colloidal particles derives from the dissociation of strong acid groups, introduced during the sphere synthesis, resulting in a negatively charged surface surrounded by a diffuse counterion cloud which extends into the medium.[10-12] When the suspending medium is free from ionic impurities, the diffuse counterion cloud does not completely screen the surface charge, and a net interparticle electrostatic repulsive interaction occurs. Dejaurin, Landau, Verwey, and Overbeek (DVLO) theory has been widely used to describe this interaction between particles and is represented in the equations in (**Figure 2**).[13, 14] As the distance between particles decreases, the electrostatic repulsion and the van der Waals attraction both become stronger, but the van der Waals

attraction increases more dramatically and at small distances the particles will irreversibly aggregate. The addition of ionic species to a particle suspension decreases the Debye-layer thickness, weakens the electrostatic repulsion between particles, and causes the overall interaction potential energy to drop.

The crystal structure and lattices parameters of the polystyrene sphere dispersions depend on sphere number density. Previous studies of polystyrene sphere dispersions indicate a face-centered cubic structure at high sphere concentrations and body-centered cubic structure at lower concentrations (**Figure 3**). At low ionic strengths (< 1μM NaCl) and high particle concentrations ($\sim 10^{13}$ cm^{-3}), the system assumes a minimum energy configuration and the colloidal particles self-assemble into a macroscopic crystal, which is either body-centered cubic (bcc) or face-centered cubic (fcc).[5, 9, 15-19]

The crystalline phases of colloidal dispersions are manifested by iridescent colors. These iridescent colors derive from Bragg diffraction from ordered layers of spheres (**Figure 4**).[20]

1)
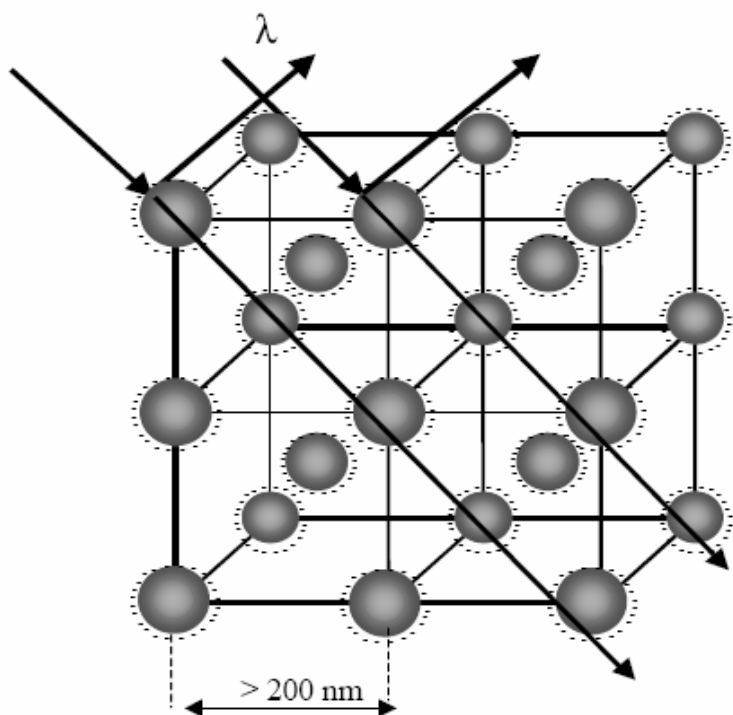
Figure 1 Self-assembly of a body-centered cubic CCA. At low ionic strengths repulsion between monodisperse, highly charged colloidal particles forces the colloidal spheres into a minimum energy configuration, which is either a body- or face-centered cubic lattice

(a)

Potential Energy of Interaction

(b)

charge

dielectric constant

sphere radius

$$U(r) = \frac{Z^2 e^2}{\varepsilon} \left[\frac{e^{\kappa a}}{1 + \kappa a} \right]^2 \frac{e^{-\kappa r}}{r}$$

Debye Layer Thickness

(c)

dissociated ions

Boltzmann's constant

ionic impurities

$$\kappa^2 = \frac{4\pi e^2}{\varepsilon k_B T} \left(n_p Z + n_i \right)$$
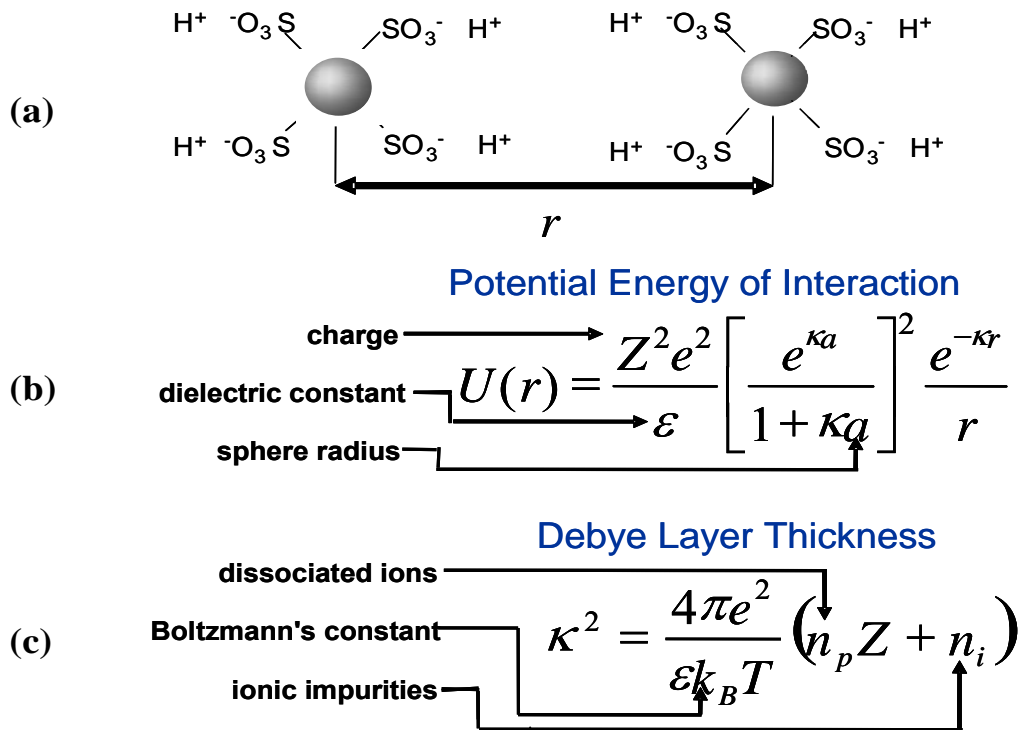
Figure 2 : (a) Sulfonate groups provide surface charge to particles separated by a distance *r*. (b) The equation for potential energy of interaction is a function of the distance between particles. (c) The equation for Debye layer thickness relates ionic impurities to the potential energy of interaction.[14]
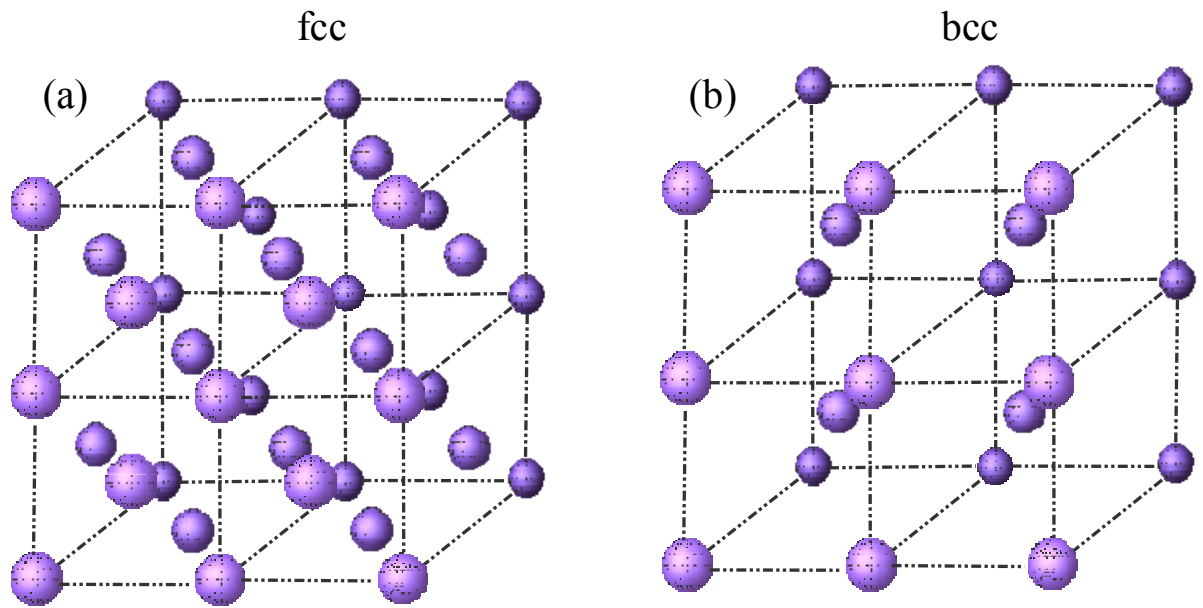
Figure 3 : The (a) fcc and (b) bcc crystal lattice form when the particles self-assemble into an array. The concentration of ionic species and the particle density determines which structure will assemble.

The Asher group has developed CCA materials which diffract light in the visible spectral region, generally using colloidal particles of ~120 nm diameter. The colloidal particles may be composed of inorganic materials such as silica, or organic polymers such as polystyrene, poly(methyl methacrylate) or poly(N-isopropyl acrylamide). Since the periodicity of the CCA is on the order of 50 to 500 nm, the CCA diffracts ultraviolet, visible or near infrared light, depending on the lattice spacing and in agreement with Bragg's law **: mλ= 2nd sinθ** where **m** is the order of diffraction, λ is the diffracted wavelength in a vacuum, **n** is the refractive index of the system (solvent, hydrogel and colloids), **d** is the spacing between the diffracting planes, and θ is the glancing angle between the incident light propagation direction and the diffracting planes **(Figure 4).** The interparticle spacing can be varied from a close packed system to a system where the interparticle spacings are many times the particle diameter.[21-26]

The Bragg diffraction of light from these colloidal crystals is very efficient, and is analogous to the diffraction of X-rays from atomic crystals. Colloidal crystals can be prepared to diffract near the UV, visible, and near IR regions merely by diluting a concentrated suspension. The diffraction bands are narrow (< 10 nm), and light which is not diffracted transmits through the crystals. The Asher group has developed optical rejection filters based on these colloidal crystals.[3, 5, 7]
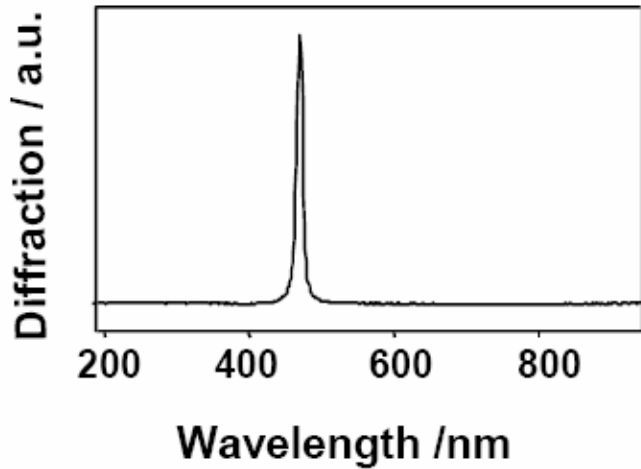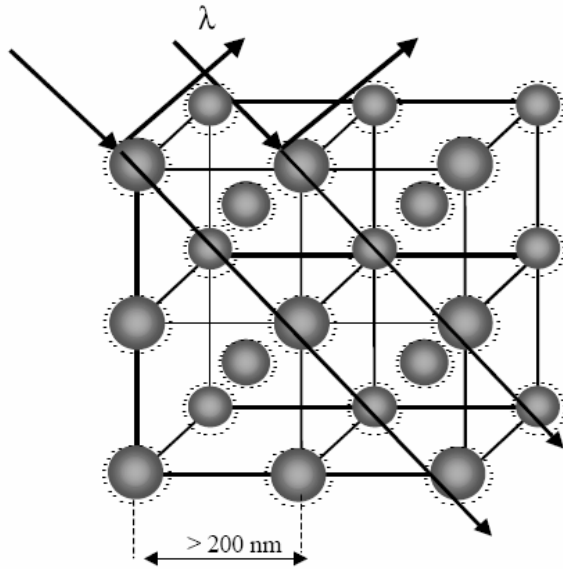
$$m\lambda = 2nd\sin\theta$$

Figure 4: Self-assembly of a body-centered cubic CCA. At low ionic strengths, repulsion between monodisperse, highly charged colloidal particles forces the colloidal spheres into a minimum energy configuration, which is either a body- or face-centered cubic lattice. CCA diffracts visible light. The spectrum is measured with a CCD spectrophotometer using reflectance probe. The diffraction obeys Bragg's law.

1.2   THE POLYMERIZED CRYSTALLINE COLLOIDAL ARRAY PCCA

Since these arrays are simply particles suspended in a liquid, they are not very robust and can be easily disrupted, losing their crystalline order when shaken. Ionic impurities inside the colloidal suspension (> 1 µM) also screen the electrostatic repulsive interaction, causing disordering of the CCA, which result in reduction in intensity and then eventual loss of Bragg diffraction.   To make the system more robust, the Asher group developed methods to permanently lock the order of the CCA by embedding the CCA into a polymer network, thus making Polymerized Crystalline Colloidal Arrays (PCCAs). This results in a durable hydrogel film. The diffraction of this hydrogel is approximately at the same wavelength as it was in the liquid CCA **(Figure 5)** [26-28]

(a)

Crystalline Colloidal Array

monomer
crosslinker
initiator

Polymerized
Crystalline Colloidal Array
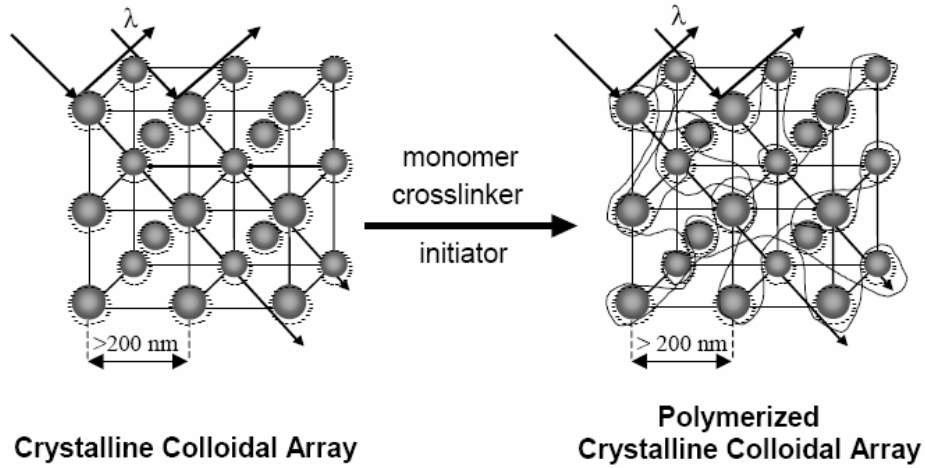
(b)
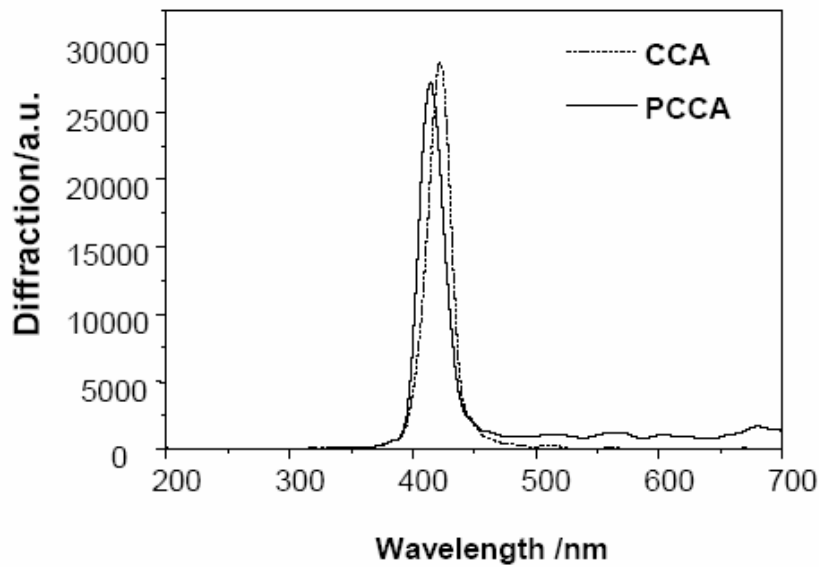
Figure 5: a)Polymerized crystalline colloidal array is developed by introducing a monomer (for example, acrylamide) and crosslinker (for example, N,N'-methylenebisacrylamide) and initiator (diethoxyacetophenome) inside the CCA liquid solution. Schematically shown is the hydrogel polymerized around the CCA. b) The diffraction spectrum from CCA and PCCA is measured with CCD spectrophotometer using reflectance probe.[28]

1.3   EXPERIMENTAL SYNTHESIS OF A PCCA

The PCCA is synthesized by dissolving acrylamide (0.08 g, 1.12 mmol, Fluka) N,N'-methylenebisacrylamide (0.005 g , 0.032 mmol, Fluka), colloid suspension (2.00g, 8% w/w dispersion, polystyrene latex spheres, 168-nm diameter) in Nanopure water, (AG 501-X8 (D) ion exchange resin, Bio-Rad) and 10% DEAP which initiates the free radical polymerization (7.7 μl, 3.84 μmol, DEAP, diethoxyacetophenone, Aldrich) in DMSO (Fisher) were mixed in a 2-dram sample vial.   The mixture is centrifuged to eliminate air bubbles generated by mixing and injected between two quartz plates separated by a parafilm spacer (125 μm-thick).   The crystalline colloidal array (CCA) self-assembles to give a diffracting liquid film.   This film is photopolymerized into a polymerized CCA (PCCA) by exposure for 2 hours to UV light from two mercury lamps with their maximum intensity at 365 nm (**Figure 6).**   The cell is opened, and the PCCA is washed thoroughly with pure water.   The PCCA is cut into four pieces and kept in pure water.

The spacing between the colloidal particles is now dependent on the properties of the surrounding polymer. This material is well suited for a wide range of applications due to the ease with which we can directly measure volume changes of the hydrogel by monitoring the CCA diffracted wavelength.   The CCA periodic structure is "locked" inside this hydrogel matrix without affecting the CCA diffraction.   The PCCA films are brightly colored due to the Bragg diffracted light from the CCA**. (Figure 7)** and **(Figure 8)** illustrates the reaction. [29, 30]
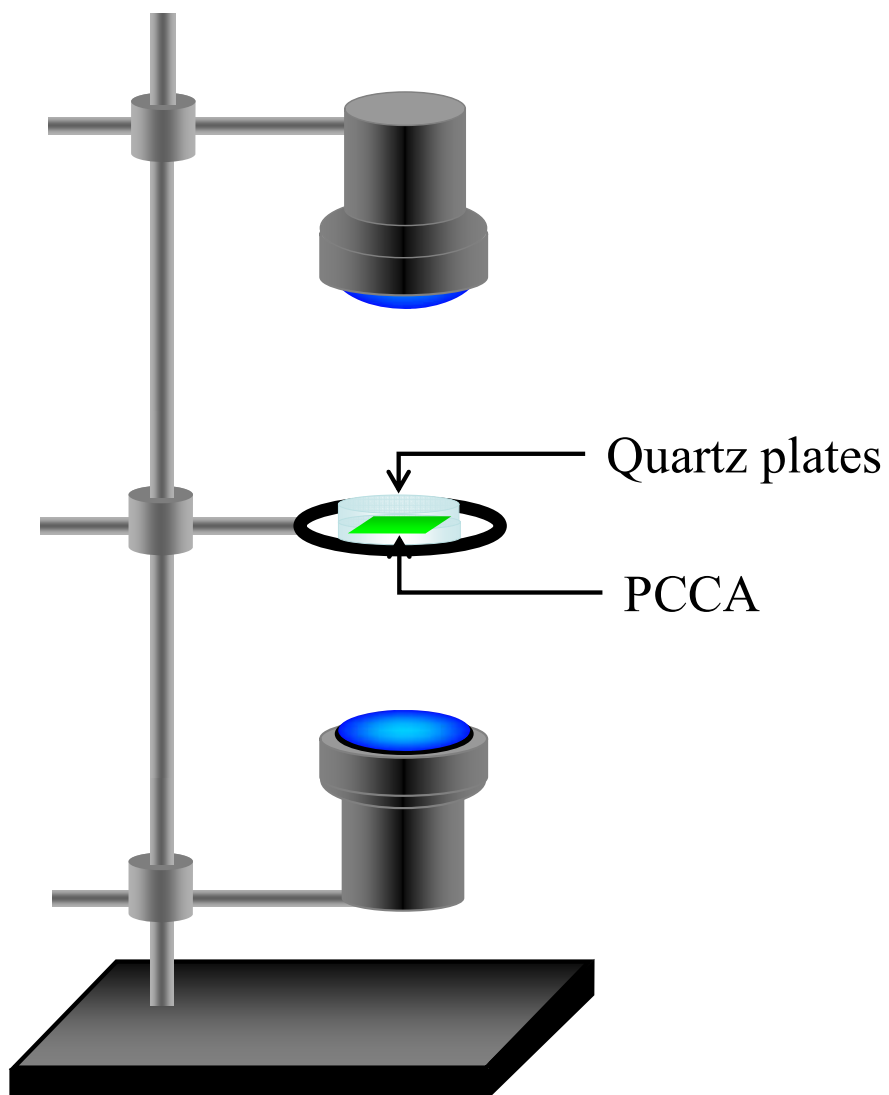
Figure 6: Apparatus for the synthesis of PCCA through UV polymerization. Two lights and careful calibration of radiative flux assure the reaction rate is equivalent on the top and bottom of the PCCA.
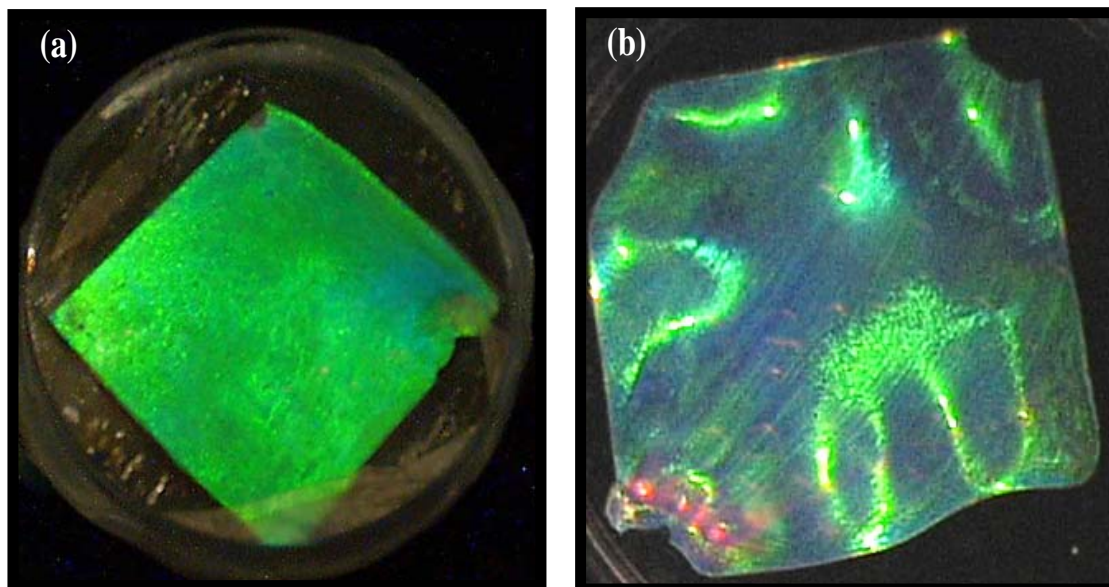
Figure 7: (a) A photograph of a CCA between two quartz plates contained by a parafilm spacer with a thickness of 125 μm. (b) After polymerization, the PCCA is structurally robust and still diffracts strongly despite having removed the quartz plates. Apparent inhomogenieties in the diffraction wavelength are the result of curves or waves in the PCCA resulting from the hydrogels flexibility *Image courtesy of Dr. Chad Reese*
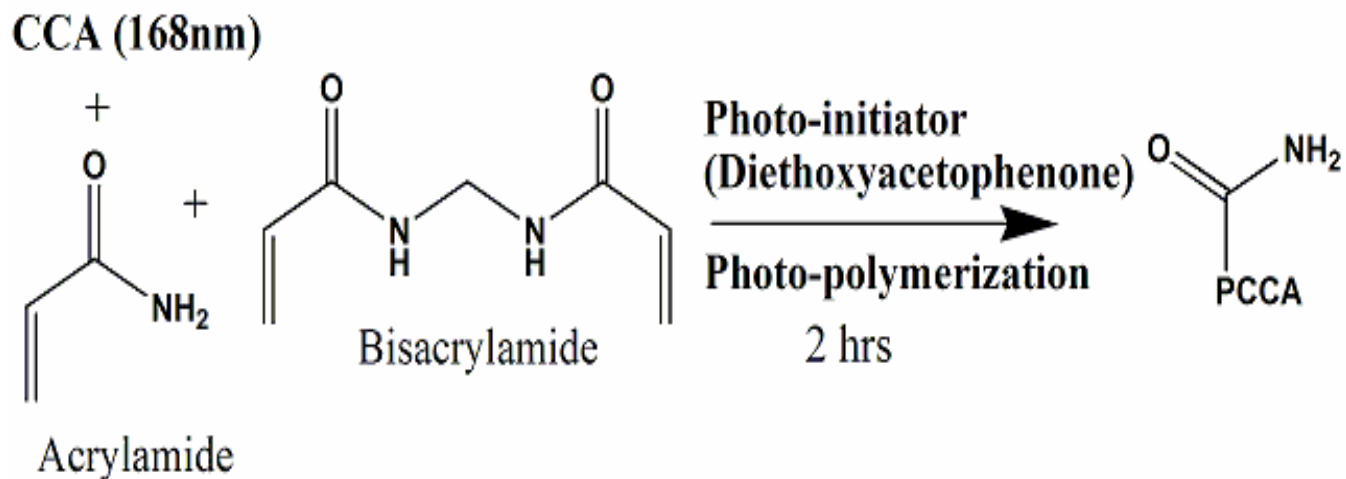
Figure 8 : The synthesis of a PCCA. The monomers and cross-links are added to a solution of the CCA. The initiator is added and the CCA is placed on the apparatus shown in Figure 6 for 2 hours

1.4   THERMODYNAMICS OF HYDROGELS

Hydrogels are cross-linked polymeric networks that are swollen with solvent. These networks change volume as their environment changes. Electrically neutral hydrogels swell in good solvents, and this tendency to swell is resisted by the elastic restoring force of the hydrogel network, which arises from the crosslinks. If a gel contains ionic groups fixed to the hydrogel polymers, the gel will swell more than will a corresponding nonionic gel in deionized water due to a Donnan-type equilibrium established by the mobile counterions of the fixed charges inside the gel and by electrolytes in the gel or its bathing solution.[31] Hydrogel volume changes can be understood from standard hydrogel swelling theories elaborated by Flory and Tanaka.[32] The equilibrium hydrogel volume is determined by the sum of three energies: the free energy of mixing of the polymer chains with the solvent medium (ΔG_{mix}), the free energy of elasticity of the cross-linked network (ΔG_{elas}), and the ionic electrostatic energy due to the Donnan equilibrium (ΔG_{ion}). The total free energy of the network (ΔG_t) gives rise to a total osmotic pressure Π_T as the volume change. **Equation 1**

$$- \partial\Delta G_T/\partial V = \Pi_T = - \partial / \partial V [\Delta G_I + \Delta G_E + \Delta G_M] = \Pi_I + \Pi_E + \Pi_M = 0 \quad \textbf{Equation 1}$$

This equation shows how the hydrogel network will respond to its chemical environment through volume changes until an equilibrium volume is reached. Free-energy changes result in osmotic pressure changes, and osmotic pressure changes result in volume changes (swelling or shrinking). The analyte for which the sensor will be designed usually dictates the mechanism of response. **Figure 9** relates the free energy of mixing, the free energy of elasticity and the ionic

14

electrostatic energy to the sum of the osmotic pressures and shows the parameters which can be influenced in order to actuate a hydrogel volume change.

$$\Delta G_{tot} = \Delta G_{mix} + \Delta G_{ion} + \Delta G_{elas}$$

$$\Pi_{tot} = -\frac{\partial \Delta G}{\partial \Delta V} = \Pi_{mix} + \Pi_{ion} + \Pi_{elas}$$

$$\Pi_M = -\frac{RT}{V_s}\left[\ln\left(1 - \frac{V_o}{V}\right) + \frac{V_o}{V} + \chi\left(\frac{V_o}{V}\right)^2\right]$$

$$\Pi_I = RT\left(c_+ + c_- - c_+^* - c_-^*\right)$$

$$\Pi_E = -\frac{RT \cdot n_{cr}}{V_m N_{av}}\left[\left(\frac{V_m}{V}\right)^{\frac{1}{3}} - \frac{1}{2}\frac{V_m}{V}\right]$$

Figure 9 : Sensors, to date, have responded to analyte through changes to χ, the Flory interaction parameter, c_+ concentration of cations inside the gel, c_- concentration of anions inside the gel, c_+^* concentration of cations outside the gel c_-^* concentration of anions ouside the gel or n_{cr}, the number of cross-links. Other parameters: R is the gas constant, N_{Av} is Avogadro number, T is the absolute temperature, Vs is the Volume of 1 mol solvent inside the hydrogel, V_0 is the volume of the dry hydrogel in pure water, V is the volume of the hydrogel in the presence of analyte, V_m is the volume of most probable configuration of the hydrogel such that stress = 0

1.4.1 Sensors using free energy of mixing ΔG_M

Flory-Huggins polymer-solvent interaction parameter, χ, is a parameter that represents the strength of the solvent-polymer interaction. A low χ leads to an increase of osmotic pressure giving rise to favorable solvent- polymer interactions and leads to greater swelling. An example of sensor utilizing free energy of mixing and causing the hydrogel to change the volume is the Photoresponsive Azobenzene Photonic Crystal developed by Kamenjicki et al.[33] Trans to cis photoisomerization of the azobenzene derivative attached to the PCCA occurs upon 365 nm excitation. The formed cis-azobenzene has a higher dipole moment which results in an increased solubility of the hydrogel in water. Formation of the cis isomer increases the free energy of mixing of the hydrogel, causing the polymer network to swell. As expected, the wavelength of the diffraction peak shift increases with the increase in cis- azobenzene concentration from 2 to 4 mM due to the increased free energy of mixing.

1.4.2 Sensor using ionic free energy ΔG_I

Ionic free energy also affects the volume of the hydrogel and can be used to make a sensor. Electrically neutral hydrogels swell into good solvents, and this tendency to swell is resisted by the elastic restoring force of the hydrogel network, which arises from the crosslinks. If a gel contains ionic groups fixed to the hydrogel polymers, the gel will swell more than will a corresponding nonionic gel in deionized water, due to a Donnan-type equilibrium established by the mobile counterions of the fixed charges inside the gel and by electrolytes in the gel or its

bathing solution.[31, 34] In addition, repulsions between charged groups will further swell the gel at high charge densities.

The Asher group has developed a photonic crystal material composed of a hydrolyzed polymerized crystalline colloidal array (PCCA) that can be used to sense pH and ionic strength. When the PCCA is hydrolyzed, some amide groups are converted to carboxyl groups, which ionize as determined by their pK_a (5.2) and solution pH. Ionization of these covalently attached carboxyl groups immobilizes counterions inside the gel. This results in an osmotic pressure, which swells the gel against its restoring elastic constant. Thus, an increased pH increases the ionization; the gel swells and the diffraction red shifts. Since ionization is complete by pH 9, further pH increases only increase ionic strength which attenuates the Donnan potential on the PCCA. This decreases the osmotic pressure and shrinks the gel. At pH lower than 7 the hydrogel shrinks (resulting in a blue-shift of the diffraction) as the pH is reduced. The shrinking is due to the acid groups being protonated. As the groups are protonated, the difference in concentration of ions inside and outside the gel is reduced. The shrinking of the IPCCA is driven by water leaving the IPCCA in response to the osmotic pressure altered by a change in ion distribution [35].

Another example of IPCCA of Donnan potential type sensor in low ionic strength is the Pb^{2+} sensor. A crown ether acryloylamidobenzo-18-crown-6 (AAB18C6)[1, 36] is attached to the PCCA as a molecular recognition agent for Pb^{2+}. As the crown ether complexes Pb^{2+} the hydrogel become positively charged. This results in the formation of an ionic gel, in which the bound Pb^{2+} immobilizes its counterions and creates a Donnan equilibrium osmotic pressure for low ionic strength solutions. This osmotic pressure swells the gel and red shifts the diffraction. The Donnan potential is attenuated in high ionic strength solutions. Thus, the hydrogel swelling is reduced, which decreases the responsivity of the PCCA to high concentrations of Pb^{2+}.[37]

These sensing motif do not operate in high ionic strength solution since the Donnan potential becomes swamped at high ion concentration, which limits the application of sensors based on ionic free energy.

1.4.3 Sensor using elastic free energy ΔG_{elas}

The gel volume changes is due to increase of the density of cross-links holding the hydrogel network which increase the restoring force and cause the gel to shrink.[32] The sensor based on elastic free energy offers the advantage of working in high ionic strength. For example, Asher et al [38] has developed an aqueous metal cation sensor using 8-hydroxyquinoline group attached to the PCCA using EDC as coupling agent. Metal cations such as Cu^{2+}, bind to 8-hydroxyquinoline groups covalently attached to the PCCA. At low metal concentrations ($< \mu M$), the cations form bisliganded complexes with two 8-hydroxyquinolines that cross-link the hydrogel and cause it to shrink, which blue shifts the photonic crystal diffraction. These bisliganded cross-links break at higher cation concentrations due to the formation of monoliganded cation complexes. This red shifts the diffraction due to the swelling of the gel.

Alexeev. et al [39] have developed new photonic crystal glucose-sensing hydrogel material that can determine physiologically relevant concentrations of glucose at the ionic strengths typical of bodily fluids. The CCA are locked in polyacrylamide-poly(ethylene glycol) (PEG) hydrogel, or a polyacrylamide-15-crown-5 hydrogel, with pendent phenylboronic acid groups. They utilize a new molecular recognition motif, in which boronic acid and PEG (or crown ether) functional groups are prepositioned in a photonic crystal hydrogel, such that glucose self-assembles these functional groups into a supramolecular complex. The formation of the complex results in an increase in the hydrogel cross-linking, which blue shifts the photonic crystal

diffraction. The visually evident diffracted light shifts across the visible spectral region over the physiologically important glucose concentration ranges.

In summary, the equilibrium volume of the gel depends on the balance of free energy of mixing, elastic free energy and free energy due to ionic interactions, as shown in (**figure 10).**[32]

$$\mathbf{G_{tot} = G_{mix} + G_{ion} + G_{elas}}$$
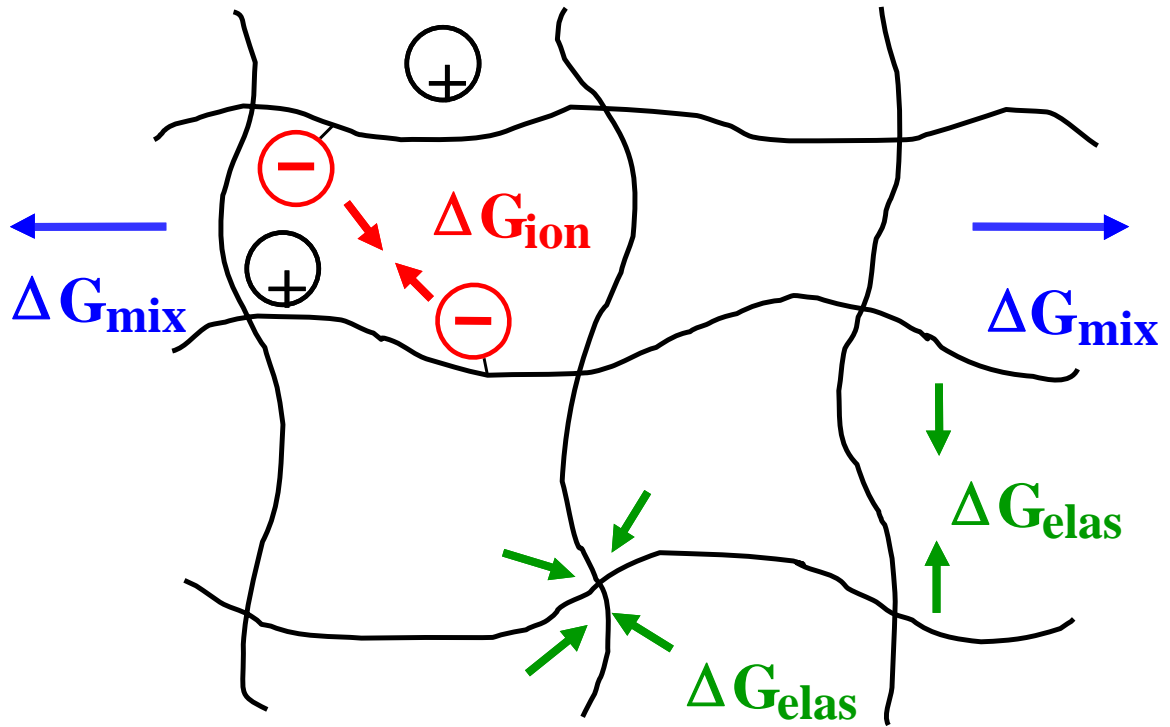
Figure 10: The forces that determine the equilibrium volume of a hydrogel can be expressed as a sum of free energies: the free energy of polymer/solvent mixing, the free energy due to ionic interactions, and the free energy of elasticity.

PCCAs have the great advantage of having a response which is easily detectable by the human eye. The sensitivity and detection range of these sensors can be adjusted by controlling the gel composition, as well as the molecular recognition agents used. Applications in medicine and environmental chemistry for these unique materials can be envisioned.

2.0 FABRICATION OF PHOTONIC CRYSTAL AQUEOUS SULFATE ANIONS SENSING MATERIALS

2.1 INTRODUCTION

There is a need for simple, inexpensive sensors for bisulfate and sulfate anions. Ammonium sulfate ($(NH_4)_2SO_4$), ammonium bisulfate ((NH_4)HSO_4) and sulfuric acid (H_2SO_4) are the most common forms of sulfate found in atmospheric particles and in nuclear waste. [40, 41] The desire to produce such anion sensor comes from an appreciation of the role they could play in radioactive waste remediation. Intensive use of nuclear energy and the Cold War era have left a worrisome legacy of radioactive waste, much of it in the form of low-activity waste (LAW). One proposed means of tackling the problem posed by these latter species involves vitrification, wherein the crude waste would be subject to evaporation and, after addition of suitable additives, high temperature glass formation. This produces "logs" that are easier to transport and less prone to leaching than other proposed storage forms. Unfortunately, the vitrification process is sensitive to slight variations in the chemical and physical parameters of the system. Sulfate anions, in particular, have been shown to influence adversely the vitrification process.[41-44]Nitrate anions, which are generally the dominant anionic species present in LAW, as well as other anions such as phosphate and chloride (present at ‹ 0.5 and 0.25–2.8 of the sulfate concentration, respectively), do not interfere appreciably with the vitrification process.[5] Recently considerable effort has been devoted to the synthesis of materials that might serve for sensing of bisulfate in

the highly basic nitrate-rich mixtures produced by pretreatment of the original radioactive waste with NaOH.[44] Other methods of separation include anion exchange,[44] extraction,[44] and precipitation.[44] While some of these approaches show considerable promise, this problem is far from being solved. Development of an inexpensive sensor that can be selectively determine sulfate anion concentration prior to vitrification is needed

In this work we attempted to develop an inexpensive new sensing material which can be used to visually determine low concentration HSO_4^- or SO_4^{2-} anions in aqueous media. The diffracted color of this sensor material would depend sensitively upon the aqueous anion concentration. This sensor material would be based on our previously developed polymerized crystalline colloidal array (PCCA) photonic crystal sensing materials. These PCCA sensing materials (**Figure 11**) utilize a mesoscopically periodic array of colloid particles, [5, 9, 11, 20, 23, 45]polymerized into acrylamide hydrogel to diffract light in the visible spectra region.[31, 35, 36, 38, 39, 46, 47] This PCCA also contains a molecular recognition agent. When an analyte binds to the recognition group, it actuates a PCCA volume change in proportion to the analyte concentration. [31, 35, 36, 46, 47] The resulting diffraction wavelength shifts cause visually evident color changes. Thus, the diffracted wavelength reports on the concentration of the target analytes.

Our new sensing material will utilizes a charged amide-amine macrocyclic compound (6,21-Bis-2amino-ethyl)-3,6,9,11,18,21,24,30-octaaza-tricyclo[24.3.1.0$^{11'16}$]-triacontal (29)11(16),12,14,26(30),27-hexaene-2,10,17,25-tetraene (PyEAmNH$_2$) as a recognition molecule for sulfate anions . Charged PyEAmNH$_3^+$ binds to anions such as HSO_4^-, SO_4^{2-}**.** Thus this sensor detects the presence of sulfate anions in aqueous media.
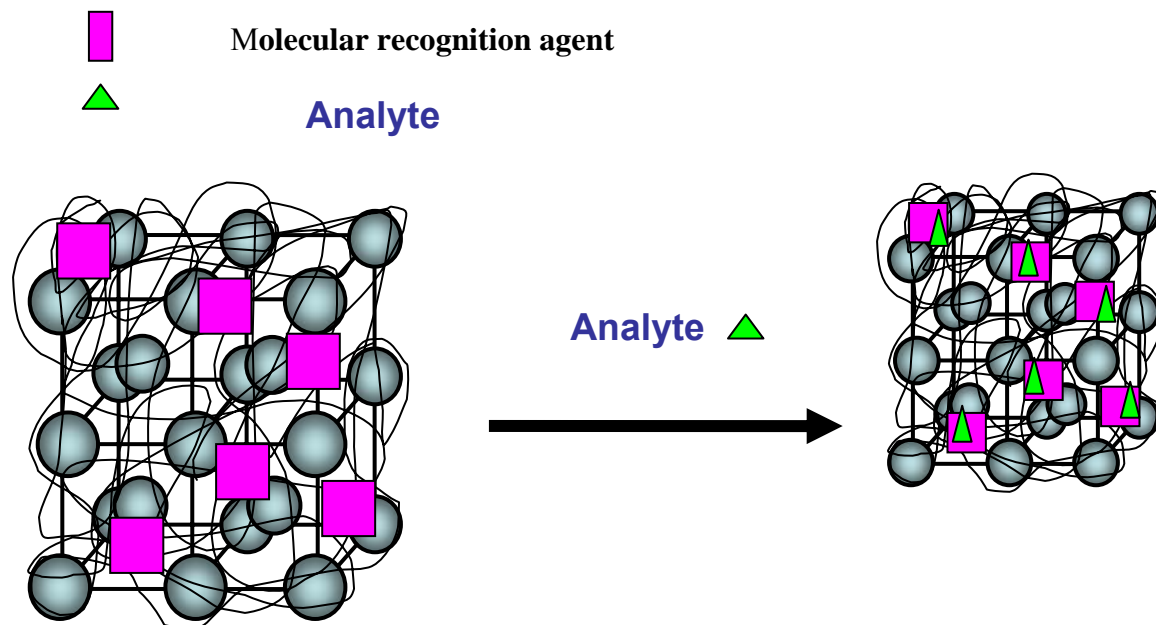
Figure 11 : Crystalline colloidal array (CCA) formed because of electrostatic repulsion between particles. The particle spacings are set such that they diffract visible light. Polymerized CCA (PCCA) formed by polymerizing a cross-linked hydrogel network around the CCA. The hydrogel is functionalized with a molecular recognition agent, which interacts with the analyte to actuate either shrinking or swelling. This alters the CCA spacing, which shifts the diffracted wavelength and changes the color.

2.2   EXPERIMENTAL

2.2.1 IPCCA preparation

Scheme 1 depicts the synthesis and functionalization of the PCCA. The PCCA was synthesized by mixing in a 2- dram sample vial, acrylamide (0.08 g, 1.12 mmol, Fluka) N,N' methylenebisacrylamide (0.005 g , 0.032 mmol, Fluka), colloid suspension (2.00g, 8% w/w dispersion, polystyrene latex spheres, 168-nm diameter,) in Nanopure water, (AG 501-X8 (D) ionexchange resin, Bio-Rad) and 10% DEAP (7.7 µl, 3.84 µmol, DEAP, diethoxyacetophenome, Aldrich) in DMSO (Fisher). The mixture was injected between two quartz plates separated by a parafilm spacer (125 µm-thick). The crystalline colloidal array (CCA) self assembles to give a diffracting liquid film. This film was photopolymerized into a polymerized CCA (PCCA) by exposure for 2 hours to UV light from two mercury lamps with their maximum intensity at 365 nm. The cell was opened, and the PCCA was washed thoroughly with pure water. The PCCA was cut into four pieces and kept in pure water.
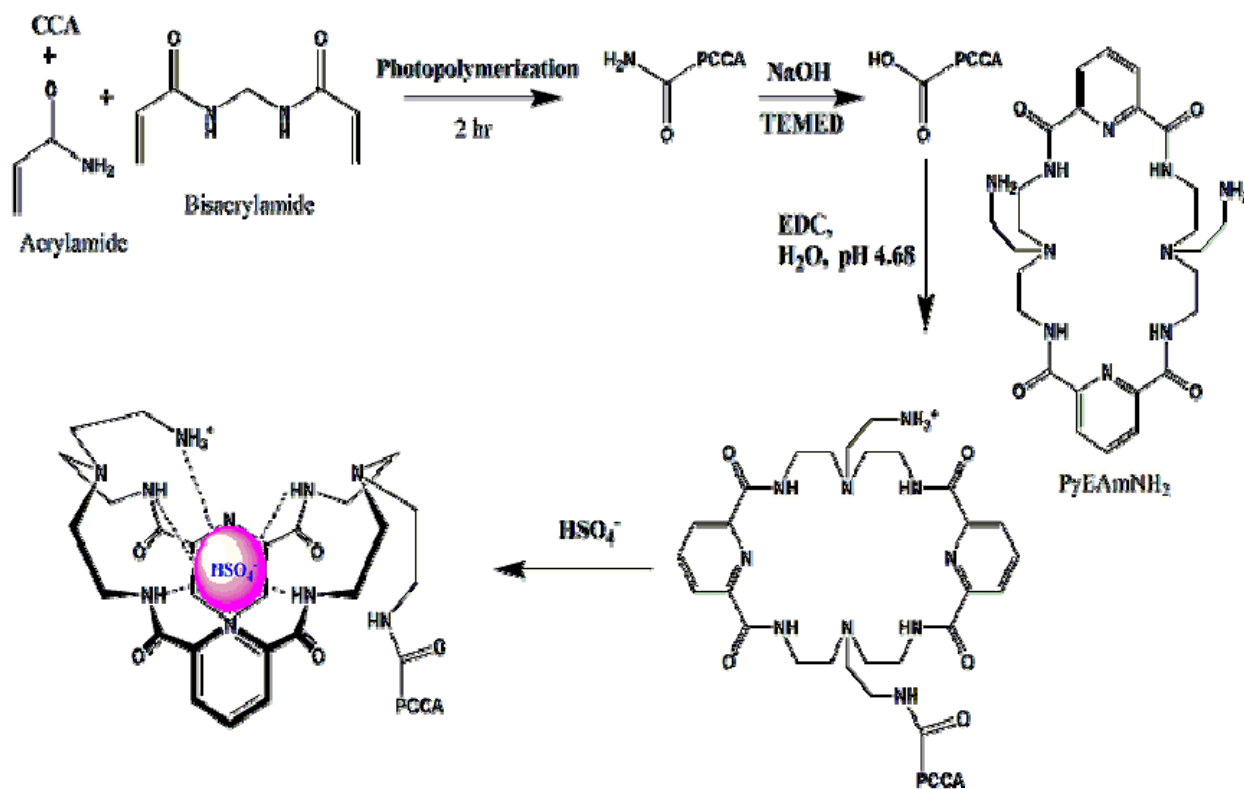
Scheme 1: chemistry of attaching the recognition molecule (PyEAmNH$_2$) to the PCCA.

The PCCA was hydrolyzed at room temperature for 5 min by placing it in (NaOH 0.1 M , Fisher) solution in 10% v/v aqueous N,N,N′,N′-tetramethylethylenediamine (TEMED; Ardrich). The hydrolyzed PCCA was stored in 0.2 M NaCl solution . The hydrolyzed PCCA was placed in a 5 ml aqueous solution of the neutral amide-amine macrocyclic compound (6,21-Bis(-2amino-ethyl)-3,6,9,11,18,21,24,30-octaaza-tricyclo[24.3.1.0^{11,16}]-triacontal   (29)11(16),12,14,26 (30),27-hexaene-2,10,17,25-tetraene (PyEAmNH$_2$, 0.0050 g, 1.8 mmol, University of Kansas) and 1-ethyl-3(3- dimethylaminopropyl) carbodiimide hydrochloride (EDC; 0.0043 g, 4.5 mmol, Pierce) for 30 min. The EDC was used as coupling agent between the hydrolyzed PCCA and the recognition molecule (PyEAmNH$_2$).

26

Pierce) for 30 min. The EDC was used as coupling agent between the hydrolyzed PCCA and the recognition molecule (PyEAmNH$_2$).

2.2.2 Attachment of recognition element (PyEAmNH$_2$) to PCCA.

The attachment of the recognition molecule (PyEAmNH$_2$) to the PCCA was monitored by comparing UV-visible absorption spectra of PyEAmNH$_2$ attached to a blank hydrogel without the CCA particles. A series of standard aqueous solutions of 288×10^{-7} M up to 900×10^{-6} M) of PyEAmNH$_2$ concentrations was prepared. The absorption spectrum of the recognition molecule gives a peak at 278 nm. From the absorbances obtained at 278 nm we plot a curve of absorbance versus concentration of recognition molecule (PyEAmNH$_2$). The slope of the curve gives the molar absorptivity of the PyEAmNH$_2$ molecule. The molar absorptivity was used to calculate the amount of PyEAmNH$_2$ attached to hydrogel using Beer's Law.

2.2.3 Diffraction measurement

The diffraction of the IPCCA was monitored using a fiber-optic diode spectrometer with tungsten halogen light source (Ocean Optics) using a reflectance probe. The IPCCA diffraction was measured in aqueous solutions containing bisulfate anions. The bisulfate anion (HSO$_4^-$) stock solutions were prepared by dissolving Tetrabutyl ammoniumbisulfate (TBAHSO$_4$) (0.0085 g, 1 mmol, Fluka) in 25 ml of pure water. Lower concentrations were prepared by successive dilution of the stock solution.

(**Table 1 shows the calculated amount of bisulfate solution and the solution pH. Calculations are shown in appendix**.)　Carbon dioxide was excluded from the analyte concentrations studies by N_2 purging, which also served to stir the solution.

TBAHSO$_4$ concentration	pH of the solution	[SO$_4^{2-}$]　moles / L	[HSO$_4^-$] moles / L	HSO$_4^-$ moles in 8 ml solution
0.01 μM	6.0 (± 0.1)	10×10^{-9}	1.0×10^{-12}	8.0×10^{-15}
0.1　μM	5.8 (± 0.1)	10×10^{-8}	2.0×10^{-11}	1.6×10^{-15}
1　　μM	5.6 (± 0.1)	10×10^{-7}	3.0×10^{-10}	2.4×10^{-14}
10　　μM	5.0 (± 0.1)	10×10^{-6}	1.0×10^{-8}	8.0×10^{-11}
50　　μM	4.0 (± 0.1)	5.0×10^{-5}	5.0×10^{-7}	4.0×10^{-11}
100　μM	3.8 (± 0.1)	9.8×10^{-5}	1.6×10^{-6}	1.3×10^{-10}
250　μM	3.4 (± 0.1)	2.4×10^{-4}	6.0×10^{-6}	4.8×10^{-10}

Table 1: Bisulafte (HSO$_4^-$) solution concentrations and pH

The IPCCA, when prepared, is extremely sticky and adheres to the polystyrene cell surface. The free IPCCA surface is now situated for exposure to the sample solution. The pure water bathing the IPCCA was replaced with an aqueous solution containing a defined analyte concentration (**Table 1**). The response time of the IPCCA to each anion concentration (the time required for diffraction peak to reach a steady state) depends on anion concentration. The response time is longest (15 min) for the lowest anion concentration but considerably shorter for

higher concentration (3 min). We waited between 30 to 20 min to ensure the equilibrium before measuring the diffraction maximum. After treatment with the highest anion concentration solution, the IPCCA was washed four times for at least 30 min with 8 ml of pure water. After washing was completed, the IPCCA was stored in pure water.

2.3   RESULTS AND DISCUSSION

2.3.1 Determination of bound PyEAmNH$_2$

As shown in (**Figure 12**) the absorption spectrum of the recognition molecule at different concentration gives peaks at 278 nm and 225 nm. Four UV absorption spectra were obtained in order to make a calibration curve of absorbance as function of different concentration of the PyEAmNH$_2$. The slope of the curve gives the molar absorptivity ($\varepsilon = 7.3 \times 10^3$) of the recognition molecule (**figure 1 3**).
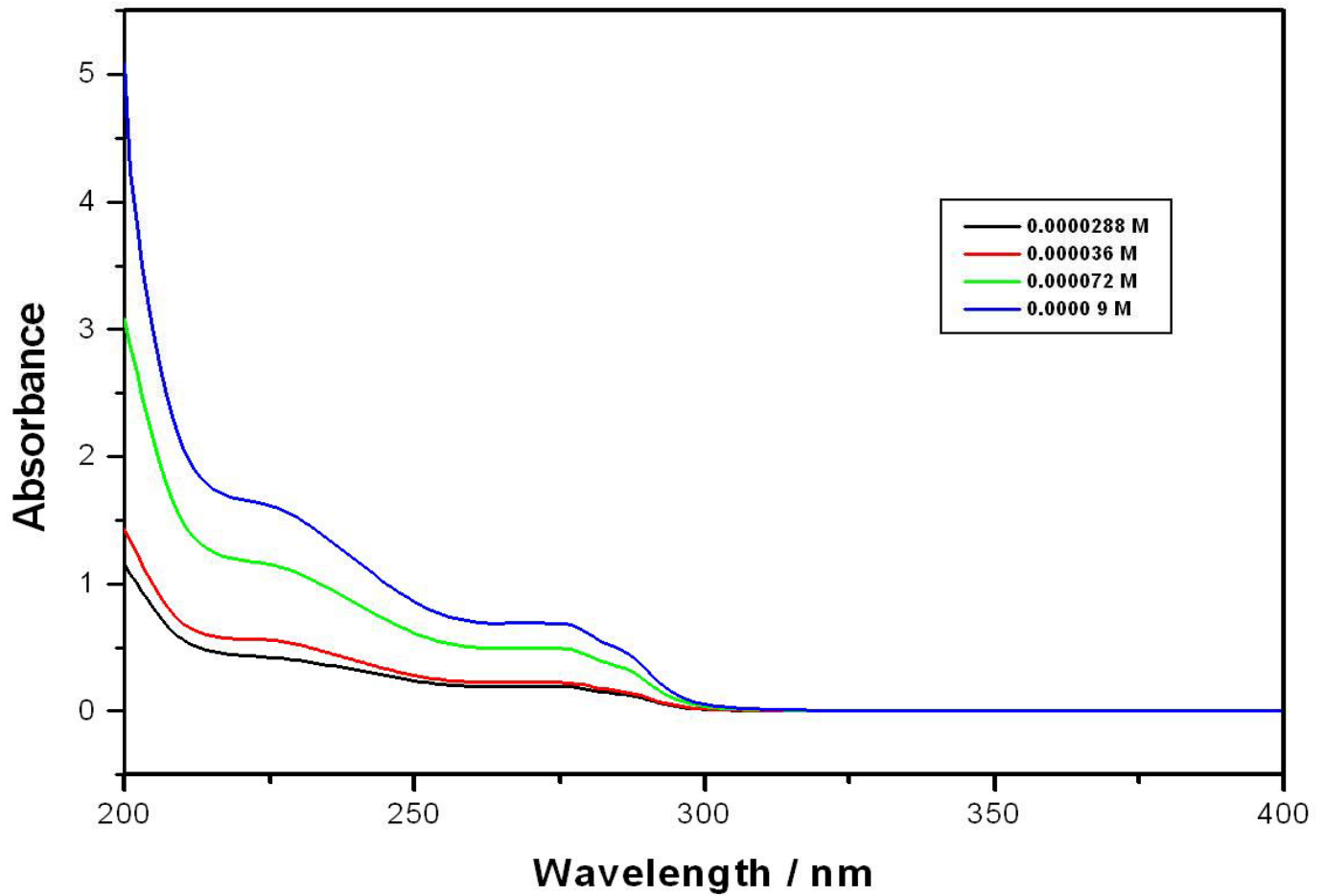
Figure 12: UV absorption spectra of free PyEAmNH$_2$ in aqueous media for different concentrations
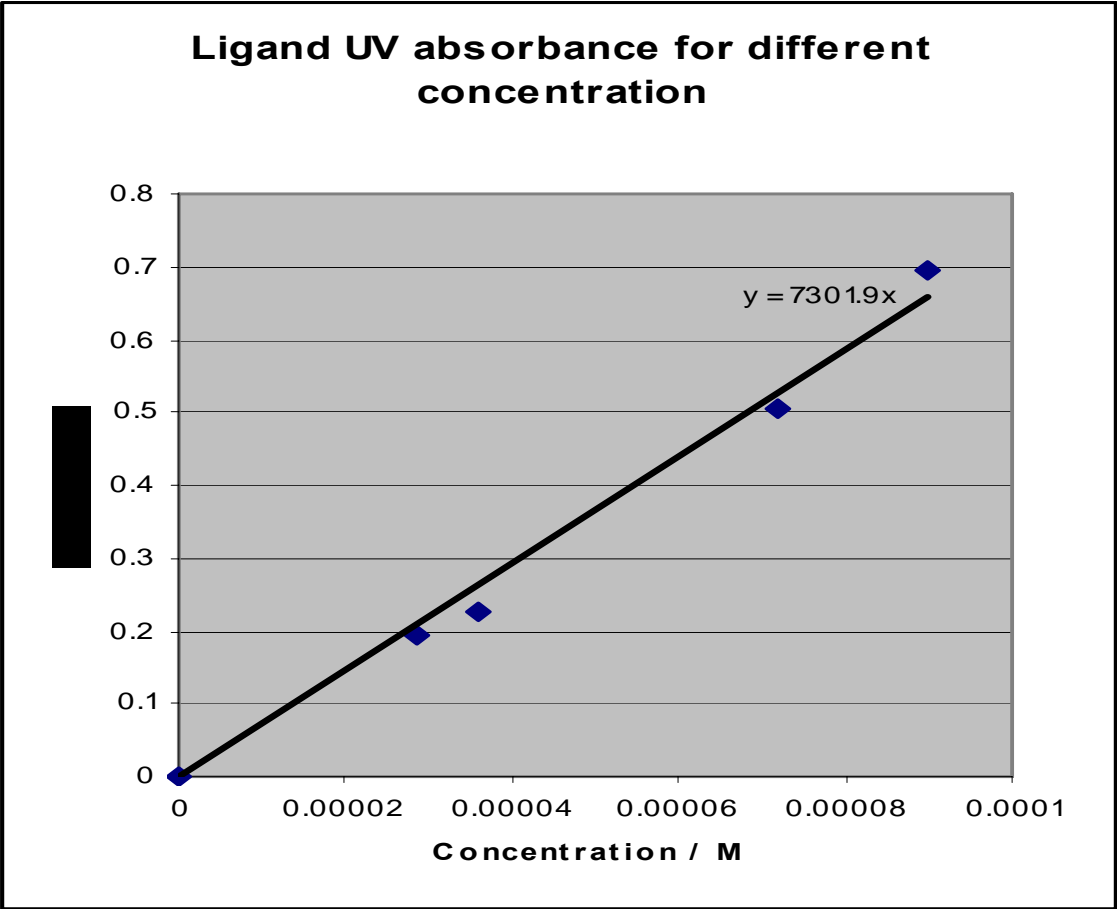
Figure 13 : Calibration curve, the slope gives the molar absorvitivity of the bisulfate recognition molecule.

Figure 14 shows the UV absorption spectra of the blank gel and the gel coupled to PyEAmNH$_2$. The IPCCA spectra shows an absorption band at 278 nm, Using Beer's low (A = εbc) we calculate the amount of PyEAmNH$_2$ bound to a 1cm × 1cm ×125 μm PCCA. The total amount of PyEAmNH$_2$ bound is 8.1×10^{-8} moles. The total amount of PyEAmNH$_2$ used for analyte detection is 2×10$^{-8.}$ moles since 1cm × 1cm ×125 μm PCCA was cut into four equal pieces. (**Calculations are shown in the appendix**)

UV spectra for a blank gel coupled with Ligand (PyEAmNH2).
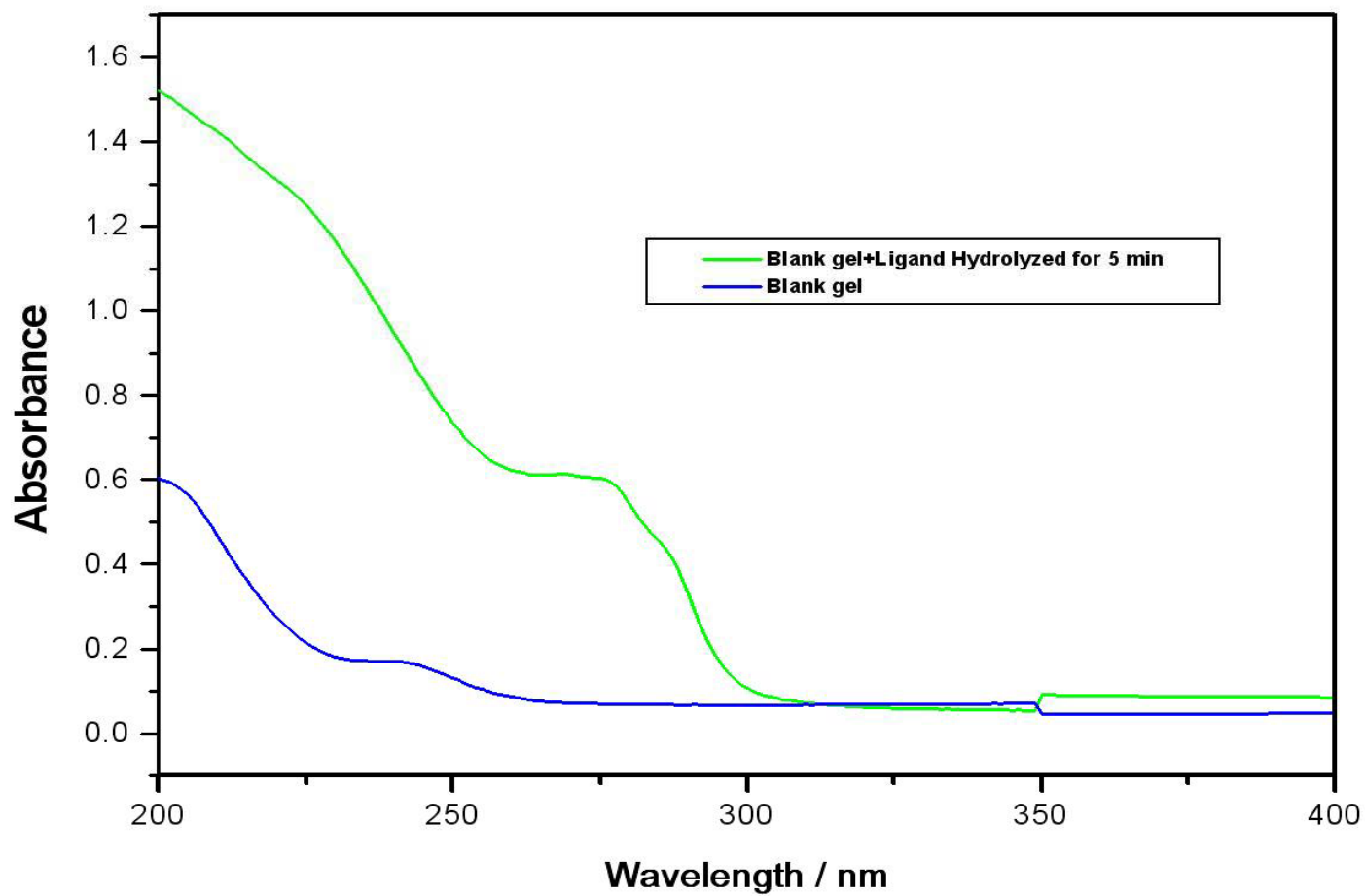
Figure 14 : UV spectra of blank gel and Blank gel coupled with the PyEAmNH$_2$

2.3.2 Response of IPCCA to TBAHSO$_4$

Working in acidic media during coupling (pH 4.68), the IPCCA becomes positively charged due to protonation of the amine group of PyEAmNH$_2$ attached to the PCCA. Upon washing with pure water, the charged IPCCA swells because of the osmotic pressure that arises from the difference in concentration of mobile ions inside and outside the IPCCA due to fixed charges on the IPCCA and their mobilized counter ions (Donnan potential). In pure water the diffraction peak occurs at 709 ($\pm$ 4) nm as illustrated in **(figure 15).**

Figure 15 : IPCCA diffraction peaks after coupling with recognition molecule ($PyEAmNH_3^+$) and after washing with pure water.

As shown in **(Figure 16)** the replacement of the pure water by 8 ml of a solution containing 8×10^{-15} moles of HSO_4^- at **pH 5.9** cause the diffraction wavelength to red shift from 713 to 723 nm. At present we do not understand the mechanism that causes this red shift.   After addition of 8×10^{-15} moles of HSO_4^- (0.01μM TBAHSO$_4$) the diffraction wavelength monotonically blue shifted as the TBAHSO$_4$ concentration increases from 0.1 μM to 250 μM. The sensor diffracts red light at 631 nm for 8×10^{-11} moles of HSO_4^- at **pH 5.1** (10 μM TBAHSO$_4$) solution and green light at 568 nm for 4.0×10^{-11} moles of HSO_4^- at **pH 4.0** (50 μM TBAHSO$_4$). The diffraction wavelength blue shift at 521 nm and steady state is reached when 4.8×10^{-10} moles of HSO_4^- was added at **pH 3.4** (250 μM TBAHSO$_4$).   The solution was removed from the polystyrene 6 multiwell container each time after the equilibrium between the solution and the IPCCA was reached. The analyte was washed out after the experiment and this caused the diffraction wavelength to red shift back to 709 nm. The same IPCCA was used to perform other experiments described in this report.

The sensor response may results from binding bisulfate anions or result from the pH and the ionic strength changes as the HSO_4^- concentration increases. Two control experiments were performed in order to determine whether the observed blue shift is due to the IPCCA binding HSO_4^-, or if carboxylate groups from the hydrolyzed PCCA which were not substituted by the recognition molecule (PyEAmNH$_2$) during coupling are being protonated as the pH decreases and the increase of ionic strength.
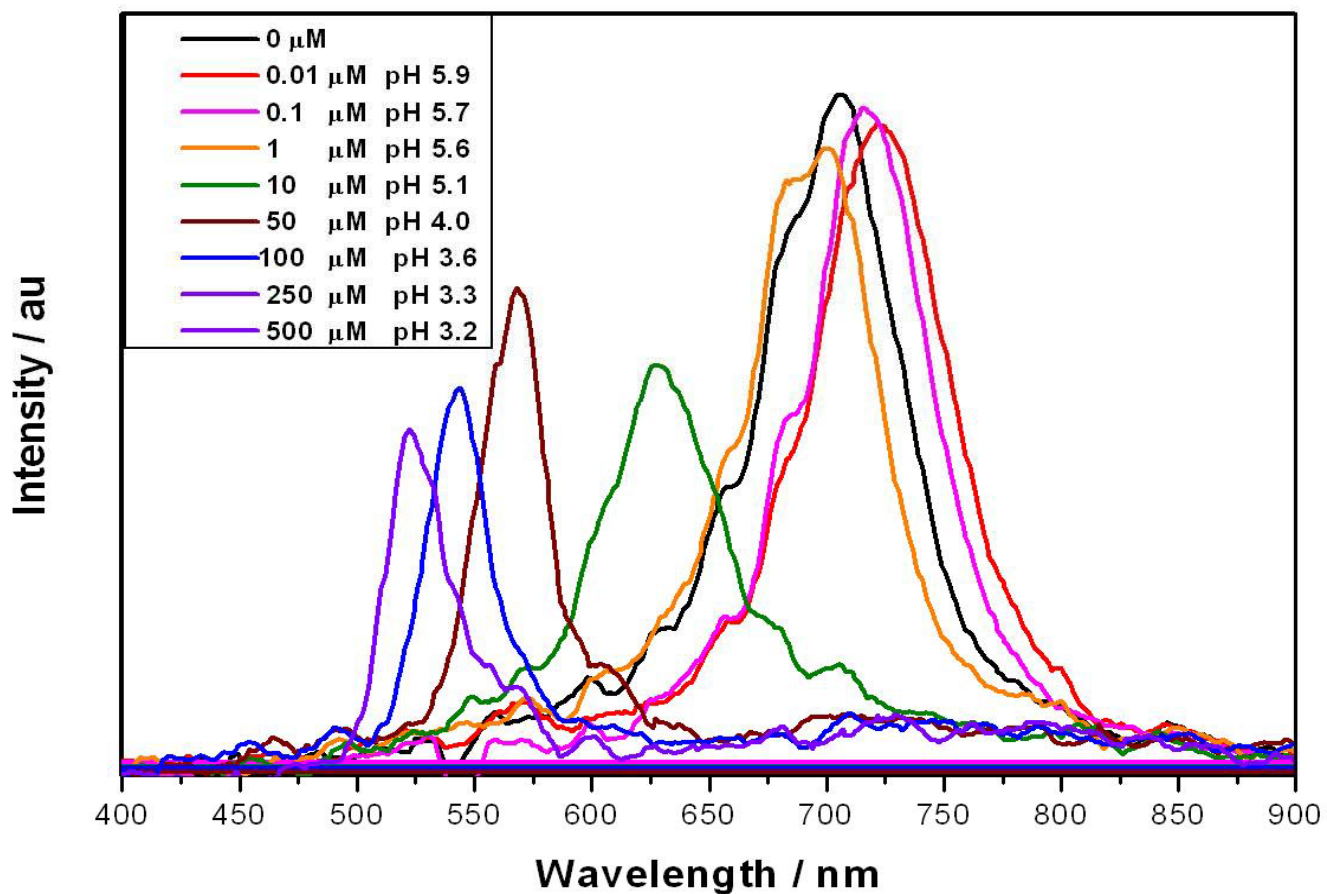
Figure 16: Bisulfate ions concentration dependence of diffraction of the IPCCA sensor in deionized water. The diffraction peaks are labeled with their sulfate ions concentrations in µM.
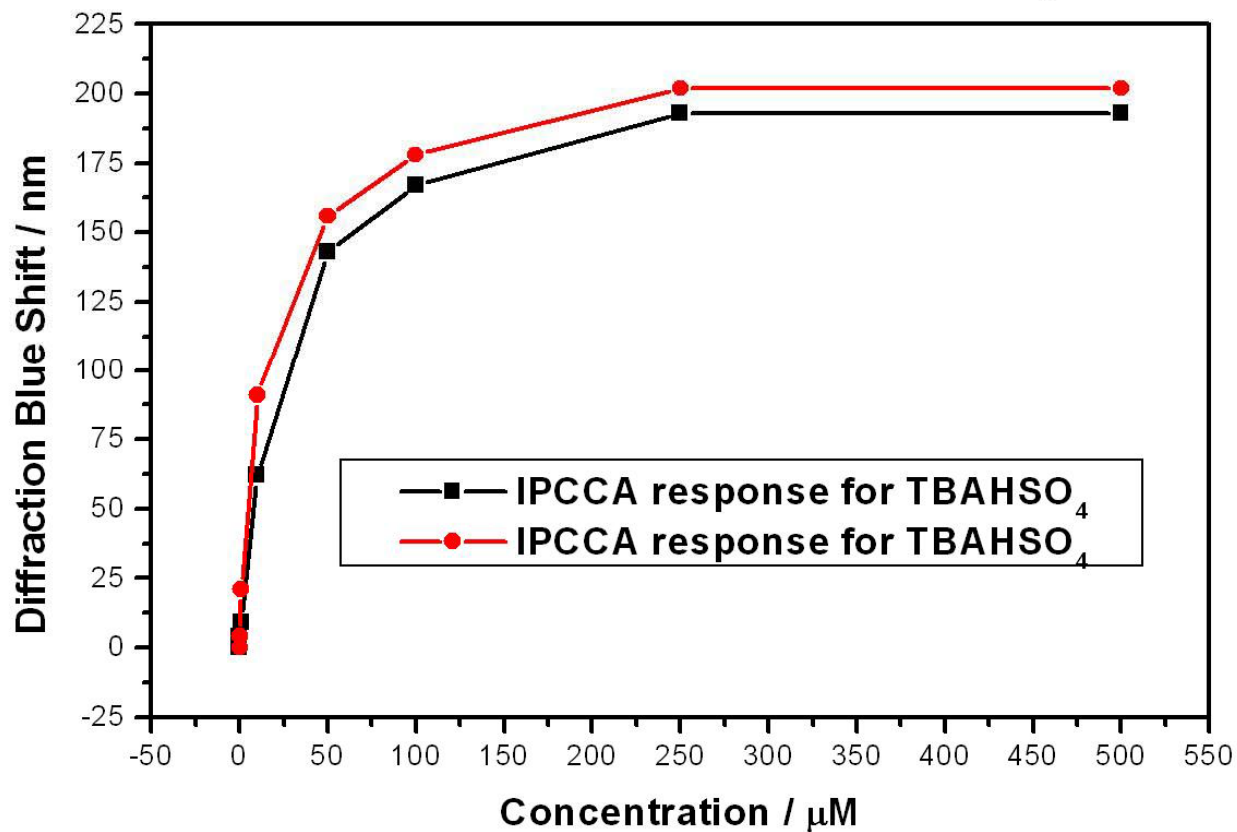
Figure 17 : Reproducibility of the IPCCA response to addition of TBAHSO₄. The diffraction wavelength blue shifted for 202 nm for the upper curve and 193 nm for the lower curve

2.3.3 The effect of ionic strength on the IPCCA for HSO_4^-

The ionic strength dependence of diffraction on IPCCA for HSO_4^- was studied by using different concentrations of NaCl in pure water. A stock solution containing 1mM NaCl was prepared, lower concentrations of the solution were prepared by successive dilution of the stock solution. Oxygen and CO_2 were excluded from the analyte concentrations studies by N_2 purging ,which also served to stir the solution. As shown in **figure 18** in the absence of NaCl the sensor gives a symmetric diffraction peak at 711 nm. From 0.01 μM to 100 μM NaCl concentrations the IPCCA shows a shift in diffraction wavelength from 710 to 656 nm . At higher concentrations the diffraction wavelength monotonically blue shifts from 656 nm to 532 nm as NaCl concentration increases from 100 μM to 20 mM.
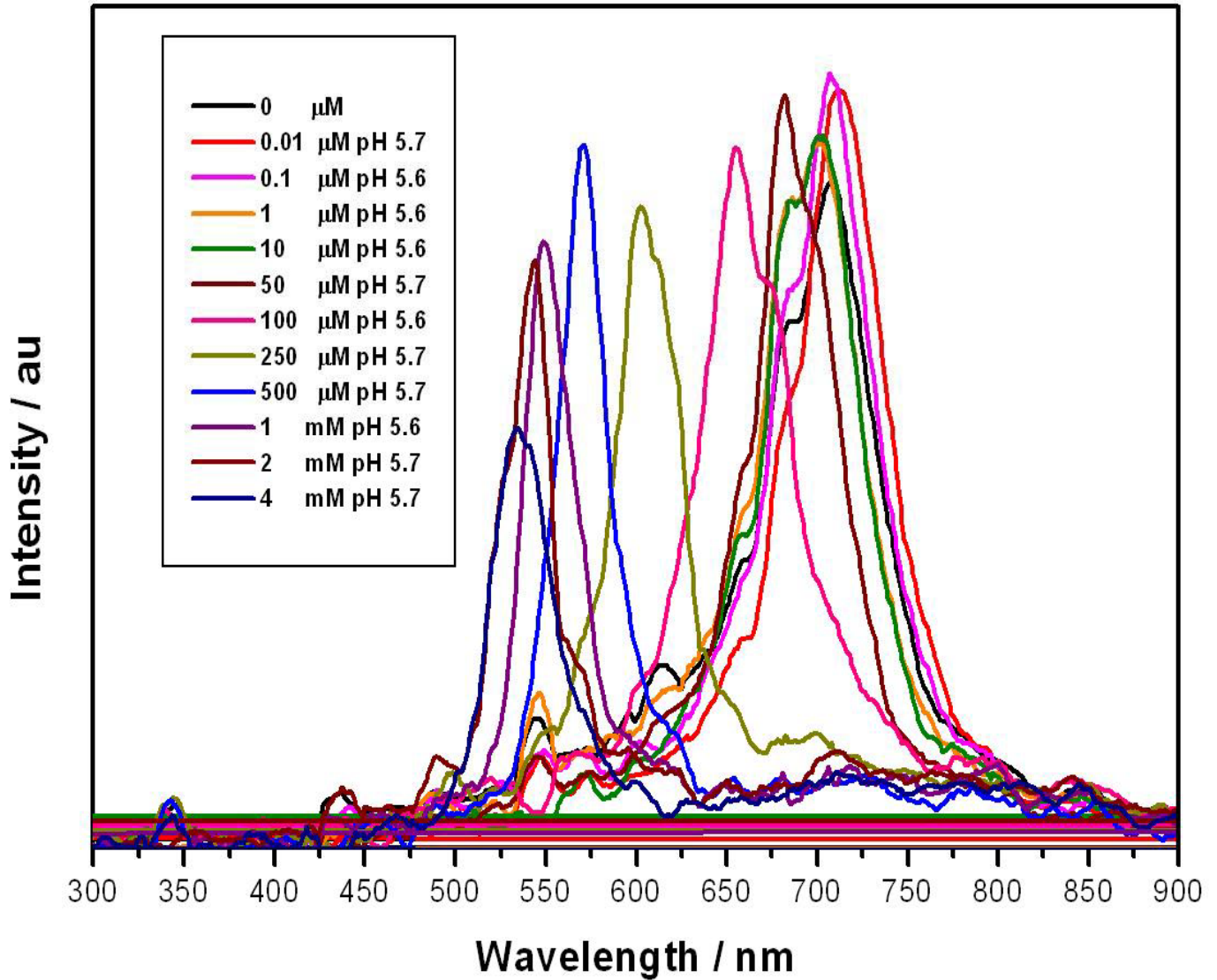
Figure 18 : NaCl concentration dependence of diffraction of the IPCCA sensor in deionized water. The diffraction peaks are labeled with their NaCl concentrations

Figure 19 shows the IPCCA response to NaCl. At lower ionic strength, from (0.01 to 100 μM) NaCl the diffraction peak blue shifts by **53 ± 3 nm** and additionally blue shifts by **126 nm** from 250 to 2000 μM NaCl. The diffraction blue shift is likely due to the increasingly high ionic strength, The Donnan pontential is attenuated in high ionic strength solution. The volume of the IPCCA is decreased, and the blue-shifted diffraction steady state is reached at 2000 μM NaCl.

IPCCA response to different concentrations of NaCl in DI water

53 nm for 100 μM

NaCl; pH is : 5.6

Diffraction wavelength / nm
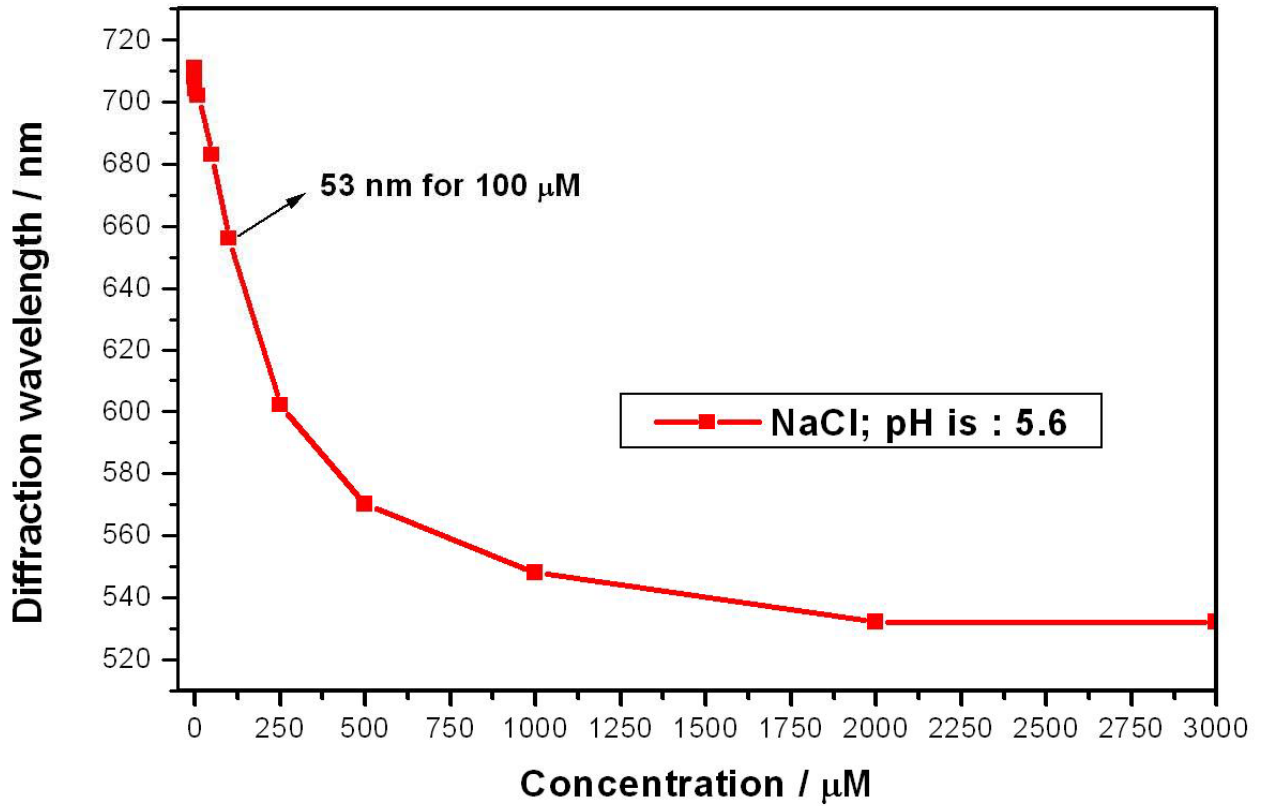
Concentration / μM

Figure 19 : Response of the IPCCA to varying concentration of NaCl. The diffraction
wavelength blue shifted as the ionic strength increases and steady-state
diffraction is reached at higher ionic strength.

2.3.4 IPCCA Bisulfate Sensor pH dependence

This experiment was done in order to determine wether the response measured from the IPCCA bisulfate sensor is due to the binding of bisulfate anions to the recognition molecule (PyEAmNH$_2$) or if there were some carboxylates group from the hydrolyzed PCCA which were not substituted by the recognition molecule (PyEAmNH$_2$) during coupling that are being protonated as the pH decreases. The pH sensor was fabricated by hydrolyzing the polyacrylamide hydrogel, resulting in acrylamide groups being converted into carboxyl groups. In previous studies, these carboxyl groups were found to have a pK$_a$ of 5.2.[35] With a pK$_a$ of 5.2, they are protonated and become uncharged at pH lower than the pKa. At pH lower than 5.2 the hydrogel shrinks (resulting in a blue-shift of the diffraction peak). The shrinking is due to the acid groups being protonated. As the groups are protonated, the difference in concentration of mobile ions inside and outside the gel is reduced. The shrinking of the PCCA is driven by water leaving the PCCA in response to the osmotic pressure altered by a change in ion distribution.

In this experiment the diffraction of the IPCCA was measured in aqueous solutions of NaCl at the same **pH** values as those of bisulfate solution. NaCl was chosen as control because Cl$^-$ anions are not strongly bound by the recognition molecule (PyEAmNH$_2$) as shown in (**figure 19**), from 10 to 100 μM NaCl solutions (**pH 5.6 (± 0.1)**) the diffraction wavelength has blue shifted by 53 (± 3) nm whereby a blue shift of 168(± 8) nm is observed from 10 μM up to 100 μM TBAHSO$_4$ (**pH 5.0 ~ 3.8 (± 0.1)**) The sodium chloride stock solutions were prepared by dissolving sodium chloride salt (0.00145 g, 1 mmol, Fisher) in 25 ml of pure water. Lower concentrations were prepared by successive dilution of the stock solution. Carbon dioxide was excluded from the analyte concentration studies by N$_2$ purging, which also served to stir the solution.

As shown in (**Figure 20)** the replacement of the pure water by 8 ml of solution containing 0.01, 0.1 μM NaCl at **pH 5.9** and **5.7** respectively caused the diffraction wavelength to red shift from 712 to 723 nm. At present we do not understand the mechanism that cause the diffraction wavelength to red shift. Solutions containing 1and 10 μM NaCl at **pH 5.6** and **5.1** respectively caused the diffraction wavelength to blue shift from 723 to 570 nm. The diffraction wavelength blue-shifted to 534 nm for 100 μM NaCl at **pH 3.8** and to 521 nm when 250 μM NaCl was added at **pH 3.4**. The solutions were removed from the polystyrene 6 multiwell container each time after the equilibrium between the solution and the IPCCA was reached**.**
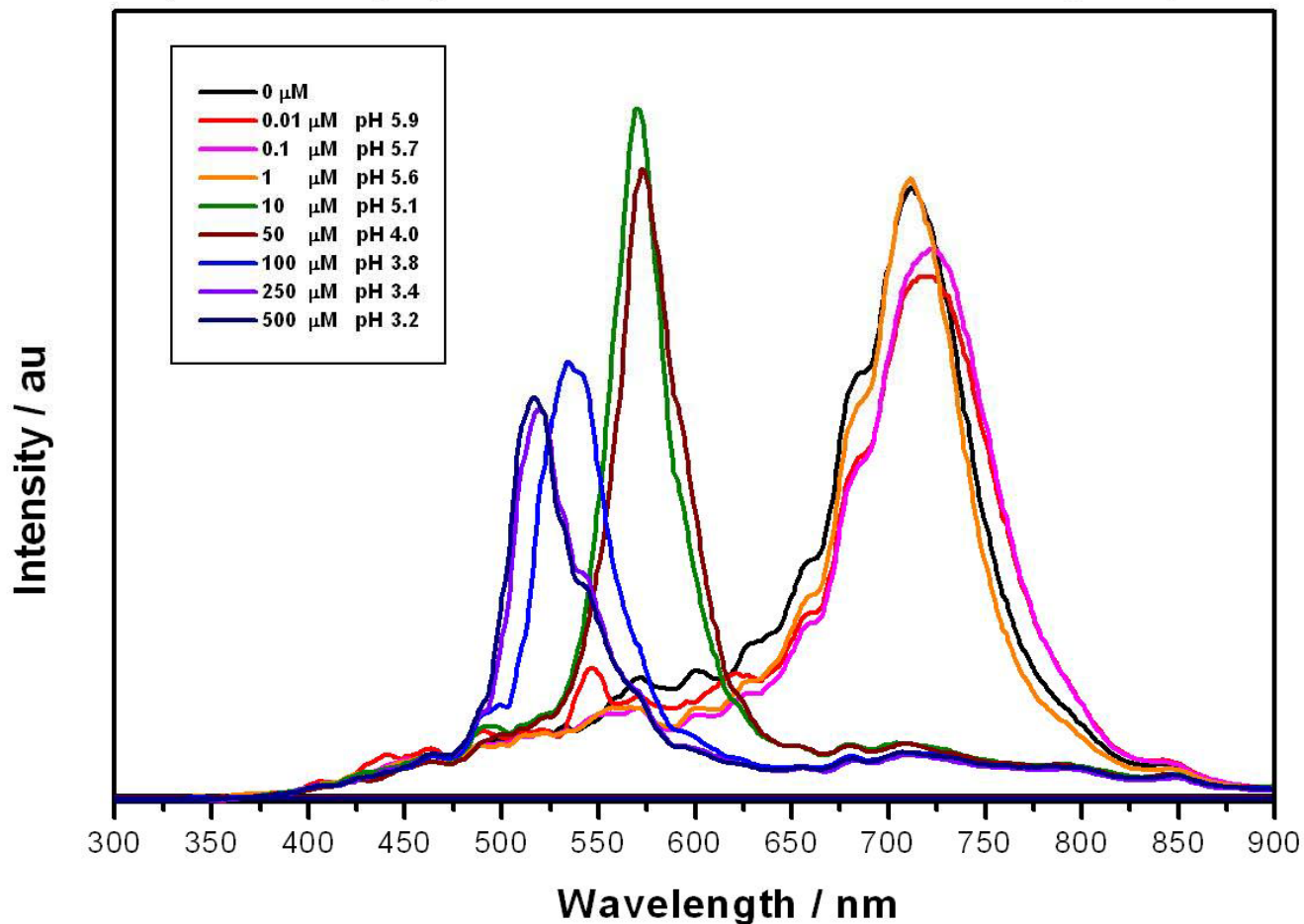
Figure 20 : Sodium chloride concentration and pH dependence of diffraction of the IPCCA sensor in deionizer water. The diffraction peaks are labeled with theirs sodium chloride concentrations in μM and pH.
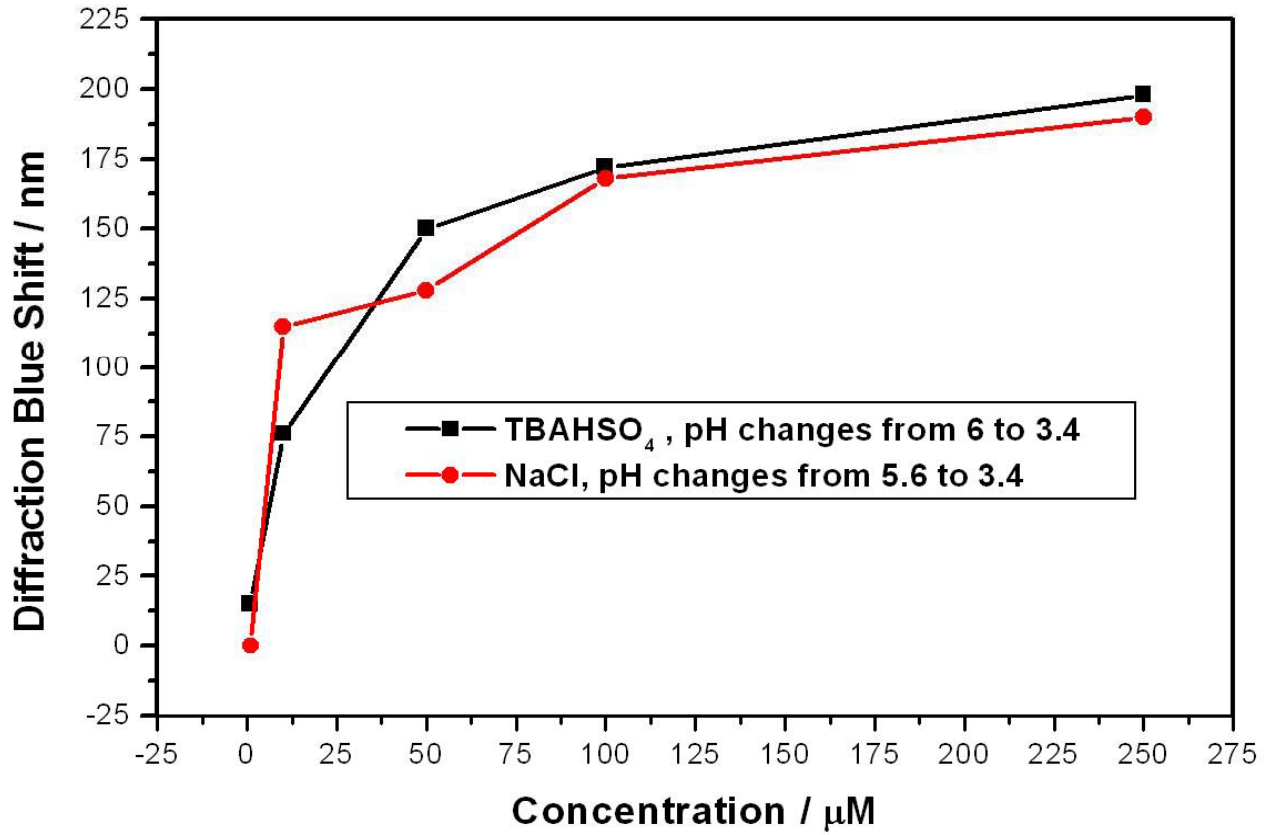
Figure 21 : Response of IPCCA to varying concentration of TBAHSO₄ versus NaCl , The sensor responds to pH and ionic strength not to bisulfate

The working range of the IPCCA for NaCl as the pH changes is illustrated in **Figure 21)**. From 10 to 100 μM NaCl solutions **(pH 5.0 ~ 3.8 (± 0.1))** the diffraction wavelength has blue shifted by **168 (± 8) nm** whereby a blue shift of **172 (± 5) nm** is observed from 10 μM up to 100 μM TBAHSO$_4$ **(pH 5.0 ~ 3.8 (± 0.1))**. These data show that the IPCCA is entirely responding to ionic strength plus the pH effect rather than binding bisulfate.

2.3.5 IPCCA response to others anions such as SO_4^{2-}, Cl^- and HPO_4^{2-}

Figure 22 illustrates the IPPCA response to different anions. From 10 to 100 μM Na_2SO_4 solutions (**pH 5.6 (± 0.1)**) the diffraction wavelength has blue shifted by **110 (± 1) nm** whereby a blue shift of **64 (± 5) nm** is observed from 10 μM up to 100 μM TBAHSO₄ **(pH 5.0 ~ 3.8 (± 0.1))**. NaCl **(pH 5.6 (± 0.1))** and Na_2HPO_4 **(pH 5.8 ~ 7.2 (± 0.1))** show a diffraction blue shift of **50 ((± 3) nm** in the range of 10 μM up to 100 μM. A window difference of **46 nm** and **60 nm** of IPCCA response between SO_4^{2-} versus HSO_4^-, Cl^-, HPO_4^{2-} respectively is observed. Comparing the ionic strength between the Na_2SO_4 and NaCl solution we calculated that the ionic strength of the Na_2SO_4 solution is three times higher than that of NaCl. This explains the origin of the same **85 nm** IPCCA response for 75 μM of Na_2SO_4 as for 225 μM NaCl. Thus the differences observed indicates that the IPCCA is not selective for SO_4^{2-} anions, rather it is due to the ionic strength increase

Figure 22 : Response of IPCCA to varying concentration of SO_4^{2-} ions versus different types of anions. The difference in IPCCA response to those anions is due their difference in ionic strength.

2.4   CONCLUSION

We tried to fabricate a novel sensing material that can determine micromolar concentration of sulfate anions in low ionic strength aqueous media. We expected that at low SO_4^{2-} or HSO_4^- concentrations (10- 100 µM) the positively charged IPCCA would be neutralized by binding SO_4^{2-} or HSO_4^- which would shrink the hydrogel network. As expected, the addition of TBAHSO$_4$ and Na$_2$SO$_4$ solutions results in diffraction blue shift of **172 (± 5) nm and 110 (± 1) nm** respectively. However, the controls experiments show that the IPCCA response results not from HSO_4^- or SO_4^{2-} binding but from increases in solution ionic strength and **pH**.

3.0   FUTURE WORK

3.1   DEVELOPMENT OF PHOTONIC CRYSTAL PHOSPHATE SENSOR

3.1.1 INTRODUCTION

There is a need for simple, inexpensive sensors for Phosphate. Phosphate is the most abundant intracellular anion. One hundredth of the body's mass is made up of phosphate. Most of this (85 %) is stored as hydroxyapetite crystals in the bone matrix. Only 15 % is metabolically active, and 14 % is stored in soft tissues as phosphate and 1 % is present in the blood. The main organ of regulation of phosphate is the kidney. In the blood, phosphate is present in multiple forms as phospholipids, as PO_4^{3-}, as HPO_4^{2-} and $H_2PO_4^{-}$[48-50].

Phosphate is involved in virtually every intracellular reaction, it is the body's source of chemical energy. Every metabolic action in the body requires chemical energy adenosine triphosphate (ATP). The high energy bonds in ATP are derived from phosphate. This is essential for muscle contractility, neuronal transmission and electrolyte transport. Phosphate is a key building block for many essential intracellular compounds nucleic acids, phospholipids, enzymes and nucleoproteins. Phosphate is the main source of intracellular buffer in the body, and is particularly important for buffering volatile acid (CO_2). Phosphate is involved in cascades within the coagulation and immune systems.[48]

The normal range for inorganic serum phosphate is generally quoted as 0.81-1.45 mM, once this concentration of phosphate become less than 0.65 mM individuals may develop hypophosphatemia [48, 50, 51] The development of Photonic Crystal Phosphate Sensor will contribute to the medical monitoring of the concentration of phosphate by utilizing cheap devices.

3.1.2 Hypothesis of Aqueous Phosphate Sensor

Cyclic voltammetric electrochemical anion recognition investigations revealed that a neutral amide containing ferrocene derivatives selectively recognize phosphate anions ($H_2PO_4^-$) in the presence of HSO_4^- and Cl^-.[52, 53] **(Table 2) illustrates electrochemical data for phosphate anion bound to the ligand .**

E_{pa} (free)[b]	360
E_{pc} (free)[b]	270
ΔE ($H_2PO_4^-$)[c,d]	100
ΔE (HSO_4^-)[c,d]	40
ΔE (Cl^-)[c,d]	< 5

Table 2: E_{pa} and E_{pc} represent the anodic and cathodic current potentials of ferrocene /ferrrocenium redox couple of the free ligand. [c] cathodic shifts in the ferrocene redox couples produced by presence of anions added as their tetrabutylammonium salts.[d] As the concentration of the anions increased the cathodic current peak potential ferrocene /ferrrocenium redox couple began to exhibit the features of an EC mechanism.[52, 53]

Proton NMR titration investigation with tetrabutylammonium salts (TBN$^+$ X$^-$, X$^-$ = H$_2$PO$_4^-$,

HSO$_4^-$, Cl$^-$) in acetonitrile indicated the receptor formed 1:1 solution complexes with H$_2$PO$_4^-$

more than other anionic guests.[52, 53] Moreover, as indicated in **Scheme 2** using the amine (-NH$_2$)

functional group of the neutral amide ferrocene derivatives we can bind the phosphate

recognition molecule to the polymerized crystalline colloidal array. After coupling the phosphate

recognition molecule to the PCCA, we will have an intelligent polymerized crystalline colloidal

array (IPCCA). This IPCCA should become a phosphate anion sensor material.

Chemistry of Phosphate Sensor
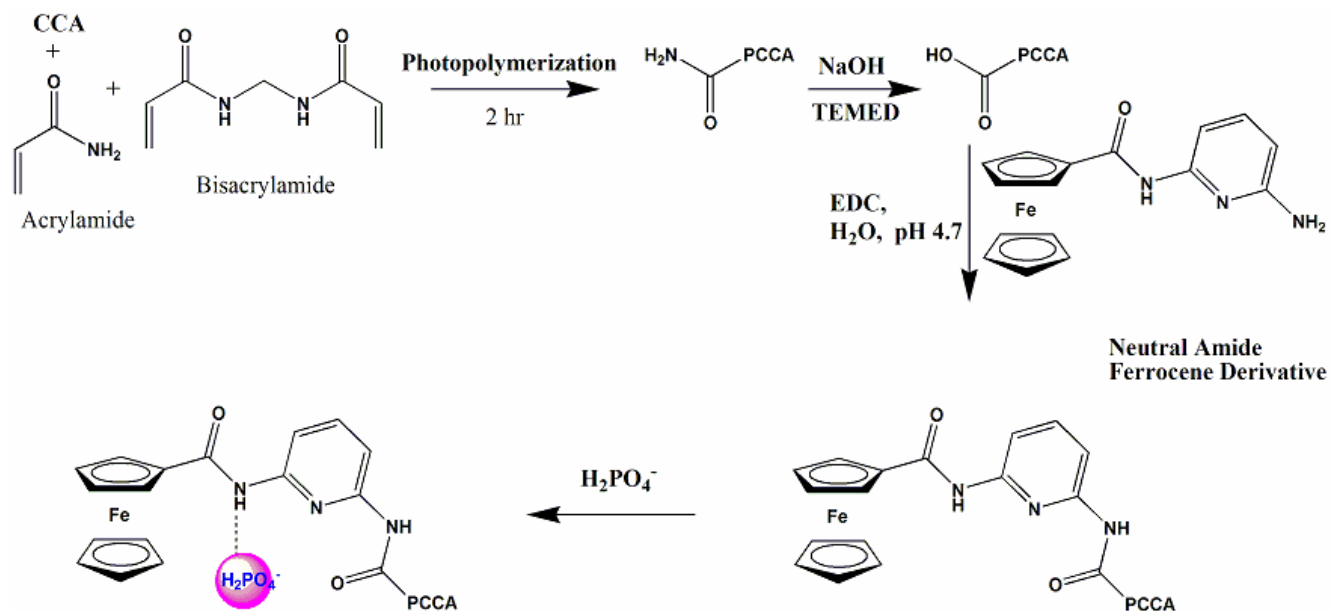
Scheme 2: chemistry of attaching the recognition molecule (Neutral Amide Ferrocene derivative) to the PCCA.

The IPPCA becomes negatively charged as it complexes phosphate anions, the negatively charged IPCCA will swell because of the osmotic pressure that arises from the difference in concentration of mobile ions inside and outside the IPCCA due to fixed charges and its mobilized counter ions inside the IPCCA.

The negative charges on the IPCCA will increase as Neutral Amide Ferrocene derivative complexes more phosphate anions which increasingly swells the IPCCA. [31, 35, 38, 39, 45] Once our phosphate sensor responds to phosphate anions in aqueous media, the next step will be to verify the IPCCA response to phosphate anions in plasma.

CALCULATION OF NUMBER MOLES OF THE RECOGNITION MOLECULE (PYEAMNH$_2$) ATTACHED TO THE PCCA

Absorbance (A) $= 0.\ 600$

Molar absorptivity (ε) $= 7.3 \times 10^3$ (moles/ L)$^{-1}$cm^1

Path length (b) $= 0.0125$cm

Concentration(C) $= A/\varepsilon\ b$

C $= 0.600\ /\ (7.3 \times 10^3$ moles/ L $\times$cm$^{-1} \times 125 \times 10^{-4}$ cm)

C $= 6.50 \times 10^{-3}$ moles/ L

Volume of the coupled blank gel $= 1$cm $\times$ 1cm $\times$ 0.0125cm

Volume of the coupled blank gel $= 1.25 \times 10^{-5}$ L

Number of mole of ligand $= 6.5 \times 10^{-3}$ moles/ L$\times$ 1.25 $\times 10^{-5}$ L

Number of mole of ligand $= 8.1 \times 10^{-8}$ moles

Volume of IPCCA used for the experiment $= 0.50$ cm $\times$0. 50 cm $\times$ 0.0125 cm

Volume of IPCCA used for the experiment $= 3.125 \times 10^{-6}$ L

Number of mole of ligand present $= 3.125 \times 10^{-6}$ L $\times$ 6.5 $\times 10^{-3}$ moles/ L

Number of mole of ligand present $= 2.0 \times 10^{-8}$ moles

CALCULATION OF THE AMOUNT OF HSO$_4^-$ PRESENT IN THE SOLUTION

pKa of HSO$_4^-$ is equal 1.92 therefore Ka = $10^{-1.92} \approx 10^{-2}$

M : moles / L

$$[HSO_4^-] = [SO_4^{2-}] \times [H^+]$$

$$10^{-2} = [SO42\text{-}] \times [H^+] / [HSO_4^-]$$

1. For 10^{-8} M of TBAHSO$_4$ pH = 6

$$10^{-2} = [SO_4^{2-}] \times 10^{-6} / [HSO_4^-]$$

$$[HSO_4^-] = [SO_4^{2-}] \times 10^{-4} \quad (1)$$

$$[HSO_4^-] + [SO_4^{2-}] = 10^{-8} \, M$$

$$[HSO_4^-] = 10^{-8} \, M - [SO_4^{2-}] \quad (2)$$

Combining line (1) and (2)

$$[SO_4^{2-}] \times 10^{-4} = 10^{-8} \, M - [SO_4^{2-}]$$

$[SO_4^{2-}] \times 10^{-4} + [SO_4^{2-}] = 10^{-8}$ M

$(x + 10^{-4} x) = 10^{-81}$

$x (1 + 0.0001) = 10^{-8}$

$x = 10^{-8}$ M / 1.0001

$x = 9.999 \times 10^{-9}$ M

$[SO_4^{2-}] = 9.999 \times 10^{-9}$ M

$[HSO_4^-] = 10^{-8}$ M - $[SO_4^{2-}]$

$[HSO_4^-] = 1 \times 10^{-12}$

2. For 10^{-7} M of TBAHSO$_4$ pH = 5.8

$10^{-2} = [SO_4^{2-}] \times 10^{-5.8} / [HSO_4^-]$

$[HSO_4^-] = [SO_4^{2-}] \times 10^{-3.8}$ (1)

$[HSO_4^-] + [SO_4^{2-}] = 10^{-7}$ M

$[HSO_4^-] = 10^{-7}$ M - $[SO_4^{2-}]$ (2)

Combining line (1) and (2)

$[SO_4^{2-}] \times 10^{-3.8} = 10^{-7}$ M - $[SO_4^{2-}]$

$[SO_4^{2-}] \times 10^{-3.8} + [SO_4^{2-}] = 10^{-7}$ M

$(x + 10^{-3.8} x) = 10^{-7}$

$x (1 + 0.00016) = 10^{-7}$

$x = 10^{-7}$ M / 1.00016

$x = 9.998 \times 10^{-8}$ M

$[SO_4^{2-}] = 9.998 \times 10^{-8}$ M

$[HSO_4^-] = 10^{-7}$ M - $[SO_4^{2-}]$

$[HSO_4^-] = 2 \times 10^{-11}$ M

3. For 10^{-6} M of TBA HSO$_4$; pH = 5.6

$10^{-2} = [SO_4^{2-}] \times 10^{-5.6} / [HSO_4^-]$

$[HSO_4^-] = [SO_4^{2-}] \times 10^{-3.6}$ (1)

$[HSO_4^-] + [SO_4^{2-}] = 10^{-6}$ M

$[HSO_4^-] = 10^{-6}$ M - $[SO_4^{2-}]$ (2)

Combining line (1) and (2)

$[SO_4^{2-}] \times 10^{-3.6} = 10^{-6}$ M - $[SO_4^{2-}]$

$[SO_4^{2-}] \times 10^{-3.6} + [SO_4^{2-}] = 10^{-6}$ M

$(x + 10^{-3.8} x) = 10^{-6}$

$x (1 + 0.00025) = 10^{-6}$

$x = 10^{-6}$ M / 1.00025

$x = 9.997 \times 10^{-7}$ M

$[SO_4^{2-}] = 9.997 \times 10^{-7}$ M

$[HSO_4^-] = 10^{-6} \, M - [SO_4^{2-}]$

$[HSO_4^-] = 3 \times 10^{-10} \, M$

4. For $10^{-5} \, M$ of TBAHSO4 pH = 5.0

$10^{-2} = [SO_4^{2-}] \times 10^{-5} / [HSO_4^-]$

$[HSO_4^-] = [SO_4^{2-}] \times 10^{-3}$ (1)

$[HSO_4^-] + [SO_4^{2-}] = 10^{-5} \, M$

$[HSO_4^-] = 10^{-5} \, M - [SO_4^{2-}]$ (2)

Combining line (1) and (2)

$[SO_4^{2-}] \times 10^{-3} = 10^{-5} \, M - [SO_4^{2-}]$

$[SO_4^{2-}] \times 10^{-3} + [SO_4^{2-}] = 10^{-5} \, M$

$(x + 10^{-3} \, x) = 10^{-5}$

$x \, (1 + 0.001) = 10^{-5}$

$x = 10^{-5} \, M / 1.001$

$x = 9.990 \times 10^{-6} \, M$

$[SO_4^{2-}] = 9.990 \times 10^{-6} \, M$

$[HSO_4^-] = 10^{-5} \, M - [SO_4^{2-}]$

$[HSO_4^-] = 1 \times 10^{-8} \, M$

5. For 5×10^{-5} M of TBAHSO$_4$ pH = 4.0

$$10^{-2} = (\, [SO_4^{2-}] \times 10^{-4} \,) / [HSO_4^-]$$

$$[HSO_4^-] = [SO_4^{2-}] \times 10^{-2} \ (1)$$

$$[HSO_4^-] + [SO_4^{2-}] = 5 \times 10^{-5} \text{ M}$$

$$[HSO_4^-] = 5 \times 10^{-5} \text{ M} - [SO_4^{2-}] \ (2)$$

Combining line (1) and (2)

$$[SO_4^{2-}] \times 10^{-2} = 5 \times 10^{-5} \text{ M} - [SO_4^{2-}]$$

$$[SO_4^{2-}] \times 10^{-2} + [SO_4^{2-}] = 5 \times 10^{-5} \text{ M}$$

$$(x + 10^{-2} x) = 5 \times 10^{-5} \text{ M}$$

$$x = 5 \times 10^{-5} \text{ M} / 1.01$$

$$x = 4.95 \times 10^{-5} \text{ M}$$

$$[SO_4^{2-}] = 4.95 \times 10^{-5} \text{ M}$$

$$[HSO_4^-] = 5 \times 10^{-5} \text{ M} - [SO_4^{2-}]$$

$$[HSO_4^-] = 5 \times 10^{-7} \text{ M}$$

6. For 10^{-4} M of TBAHSO$_4$ pH =3.8

$$10^{-2} = (\, [SO_4^{2-}] \times 10^{-3.8} \,) / [HSO_4^-]$$

$$[HSO_4^-] = [SO_4^{2-}] \times 10^{-1.8} \ (1)$$

$[HSO_4^-] + [SO_4^{2-}] = 10^{-4} M$

$[HSO_4^-] = 10^{-4} M - [SO_4^{2-}]$ (2)

Combining line (1) and (2)

$[SO_4^{2-}] \times 10^{-1.8} = 10^{-4} M - [SO_4^{2-}]$

$[SO_4^{2-}] \times 10^{-1.8} + [SO_4^{2-}] = 10^{-4} M$

$(x + 10^{-1.8} x) = 10^{-4} M$

$x = 10^{-4} M / 1.016$

$x = 9.843 \times 10^{-5} M$

$[SO_4^{2-}] = 9.843 \times 10^{-5} M$

$[HSO_4^-] = 10^{-4} M - [SO_4^{2-}]$

$[HSO_4^-] = 1.57 \times 10^{-6} M$

7. For $2.5 \times 10^{-4} M$ of TBAHSO$_4$ pH = 3.4

$10^{-2} = ([SO_4^{2-}] \times 10^{-3.4}) / [HSO_4^-]$

$[HSO_4^-] = [SO_4^{2-}] \times 10^{-1.4}$ (1)

$[HSO_4^-] + [SO_4^{2-}] = 2.5 \times 10^{-4} M$

$[HSO_4^-] = 2.5 \times 10^{-4} M - [SO_4^{2-}]$ (2)

Combining line (1) and (2)

$$[SO_4^{2-}] \times 10^{-1.4} = 2.5 \times 10^{-4}\,M - [SO_4^{2-}]$$

$$[SO_4^{2-}] \times 10^{-1.4} + [SO_4^{2-}] = 2.5 \times 10^{-4}\,M$$

$$(x + 10^{-1.4}x) = 2.5 \times 10^{-4}\,M$$

$$x = 2.5 \times 10^{-4}\,M / 1.04$$

$$x = 2.440 \times 10^{-4}\,M$$

$$[SO_4^{2-}] = 2.440 \times 10^{-4}\,M$$

$$[HSO_4^-] = 2.5 \times 10^{-4}\,M - [SO_4^{2-}]$$

$$[HSO_4^-] = 6 \times 10^{-6}\,M$$

REFERENCES

1.   Krieger, I. M.; O'Neill, F. M. *J. Am. Chem. Soc.* **1968**, *90*, 3114.

2.   Hiltner, P. A.; Krieger, I. M., *J. Phys. Chem.* **1969**, *73*, 2386.

3.   Asher, S. A. *U.S. Patents 4,627,689 and 4,632,517,* **1986**;

4.   Kesavamorthy, R.;Jagannathan, P.; Rundquist, P. A.; Asher, S. A. *J. Chem. Phys.* **1991**, *94*, 5172; 188

5.   Flaugh, P. L.; O'Donneell, S. E.; Asher S. A., *Appl. Spectrosc.* **1984**, *38*, 847.

6.   . Haacke, G.; Panzer, H. P.; Magliocco, L. G.; Asher, S. A.*U.S. Patent 5,266,238*, **1993.**

7.   Asher, S. A.; Jagannathan, S. *U.S. Patent 5,281,370*, **1994.**

8.   Asher, S. A.; Chang, S. Y.; Jagannathan, S.; Kesavamoorthy, R.; Pan, G. U.*S. Patent 5,452,123*, **1995.**

9.   Carlson, R. J.; Asher, S. A. *Appl. Spectrosc.* **1984**, *38*, 297.

10.   Hiltner, P. A.; Papir, Y. S.; Krieger, I. M. *J. Phys. Chem.,* **1971**, *75*,1881.

11.   Reese, C. E.; Guerrero, C. D.; Weissman , J. M.; Lee, K.; Asher, S.A.; *J.Coll. Int. Sci.* 2000,232, 76

12.   Aastuen, D. J. W.; Clark, N. A.; Cotter, L. K.; Ackerson, B. J. *Phys. Rev. Lett.*, **1986**, 57, 1733.

13.   Behrens, S.H.; Christl, D.I.; Emmerrzael, R.; Schurtenberger, P. Borkovec, M. *Langmuir* **2000**, 16, 2566-2575.

14.   Hiemenz, P. C.; Rajagppalan, R. *Principles of Colloid and Surface Chemistr*y, 3rd edition, Marcel Dekker, Inc., **199**7.

15.   Williams, R. and Crandall, R. S. *Phys. Lett*. 48 A, 225 (1974).

16.   Takano, T and Hachisu SJ. *Colloid Int.Sci.* **1978**;66:124.

17.   Rundquist, P. A.; Jagannathan, S.; Kesavamoorthy, R.; Brnardic, C.; Xu, S.; Asher, S. A. *J. Chem. Phys.*, **1990**, *94,* 711.

18.   Flaugh, P. L.; O'Donneell, S. E.; Asher S. A., *Appl. Spectrosc.* **1984**, *38*, 847.

19.   Hachisu, S.; Kobayashi, Y .; Kose, A. *J .Colloid Interface Sci.* **1973**, 42(2), 342-348

20.   Weissman, J. M.; Sunkara, H. B.; Tse, A. S.; Asher, S. A. *Science*, **1996**, *274,* 959.

21.   Chang, S-Y.; Liu, L.; Asher, S. A. *J. Am. Chem. Soc.*, **1994**, *116*, 6739.

22.   Chang, S-Y.; Liu, L.; Asher, S. A. *J. Am. Chem. Soc.*, **1994**, *116*, 6739.

23.   Rundquist, P. A.; Photinos, P.; Jagannathan, S.; Asher, S. A. *J. Chem. Phys.*, **1989**, *91,* 4932.

24.   Rundquist, P. A.; Kesavamoorthy, R.; Jagannathan, S.; Asher, S. A. *J. Chem. Phys.*, **1991**,*951,* 249.

25.   Tse, A. S.; Wu, Z.; Asher, A. S. *Macromolecules*, **1995**, *28,* 6533.

26.   Asher, S. A.; Holtz, J.; Liu, L.; Wu, Z. *J. Am. Chem. Soc.,* **1994**, *116,* 4997.

27.   Haacke, G.; Panzer, H. P.; Magliocco, L. G.; Asher, S. A. *U.S. Patents 5,266,238*

28.   Kamenjicki, M. PH.D. Thesis, 2004, The University of Pittsburgh

29.   Hartley, G. S. *J. Chem. Soc.,* **1938**, 633.15

30.   Robertson, J. M.; *J. Chem. Soc.,* **1939**, 232; b) Hampson, G. C.; Robertson, J. M.; *J. Chem.Soc.*, **1941**, 409.

31.   . Holtz, J. H.; Holtz, J. S. W.; Munro, C. H.; Asher, S. A. *Anal. Chem.,* **1998**, *70,* 780.

32.   Flory, P. J. *Principles of Polymer Chemistry*, Cornell University Press, Ithaca, NY, **1953.**

33.   Kamenjicki, M.; Lednev, I.K.; Mikhonin, A.; Kesavamoorthy, R.; Asher, S.A. *Adv. Funci. Mater.* **2003**, 13 (10) 774.

34.   Wang, K. L. ; Burban, J.H.; Cussler, E. L. *Adv. Polym.Sci.* **1993**;110:67.

35.   Lee, K.; Asher, S. A. *J. Am. Chem.Soc*. 2000, 122, 9534-9537.

36. Holtz, J.P.; Asher, S.A. *Nature.* **1997**;389:829-832.

37. Gopenenko, A. V. and Asher , S. A. *J.Chem.Soc.* 2005.

38. Asher, S. A.; Sharma, A. C.; Goponenko, A. V; Ward, M. M. *Anal. Chem.* 2003.

39. Alexeev VLS, A.C.; Gopenenko, A.V.; Das, S.; Lednev.I.K.; Wilcox, C.S.; Finegold, D.N.; Asher, S.A. *J.Am.Chem.Soc.* **2003**;75(10):2316-2323.

40. Jonathan, L. Sessler*[a], Evgeny Katayev,[ab], G. Dan Pantos[a] and Yuri A. Ustynyuk*[b] . *Chem. Comm.. ,* 2004,1276-1277.

41. S. O. Kang,. M. A . Hossain, D. Power and K. Bowman-James*. *Chem. Commun*., 2005,328-330.

42. Chow , J. C. and J.G Watson , *Guideline on Speciated particulate Monitoring , U S Environmental Protection Agency, Office of Air Quality Planning And Standards, Research Triangle Park , NC,* 1998.

43. J. D. Vienna, M. J. Schweiger, D. E. Smith, H. D. Smith, J. V. Crum, D. K. Peeler, I. A. Reamer, C. A. Musick and R. D. Tillotson, Report PNNL-12234, Pacific Northwest National Laboratory, Richland, Washington, Jul. 1999; (*b*) C. I. Crawford, D. M. Ferrara, R. F. Schumacher and N. E. Bibler, Report WSRC-MS-2002-00449, Westinghouse Savannah River Company, Aiken, South Carolina, Apr. 2002.

44. D. E. Kurath, J. R. Bontha, D. L. Blanchard, S. K. Fiskum and B. M. Rapko, Report PNWD-3053, BNFL-RPT-036, Rev. 0, Pacific Northwest National Laboratory, Richland, Washington, USA, Aug. 2000; (*b*) B. A. Moyer, L. H. Delmau, C. J. Fowler, A. Ruas, D. A. Bostick, J. L. Sessler, J. M. Llinares, A. Hossain, S. O. Kang and K. Bowman-James, *Supramolecular Chemistry of Environmentally Relevant Anions*, ACS Symp. Ser., American Chemical Society: Washington, D. C., in press; (*c*) S. K. Fiskum, D. E. Kurath and B. M. Rapko, Report PNWD-3050, BNFL-RPT-029, Rev. 0, Pacific Northwest National Laboratory, Richland, Washington, USA, Aug. 2000.

45. Asher, S. A.; Flaugh, L. P.; Washinger, G. *Spectroscopy.* 1996, 1(12), 26-31.

46. Asher, S. A.; Holtz. J. H.; Weissman, J. M.; Pan. G. *MRS Bull*. 1998, (October),

    44 – 50.

47. Walker, J. P.; Asher, S. A. *Anal . Chem*. 2005, 77, 1596 – 1600.

48.   Burtis,C. A.; Ashwood, E. R.*Tietz textbook of Clinical Chemistry*, W.B.Saunders Company Philadelphia, 1999

49.   N. C. Bugg and J. A. Jones. Hypophosphataemia. Pathophysiology, effects and management on the intensive care unit. *Anaesthesia* 53 (9):895-902, 1998

50.   Lung, F.; Gregor, R. ; Knox, FG, ; Oberteithner H. Factors modulating the renal handling of phosphate . *Renal Physiology* 1981; 4: 1-16

51.   Knochel, Jp. The pathophysiologilogy and clinical characteristics of severe hypophosphataemia. *Archives of Internal Medicine* 1997; 137 :203-20

52.   Beer, P.D., Chen , Z., Goulden, A. J., Graydon , A. , Stockes, S. E. and Wear, T.(1993b). *J. Chem.Soc., Comm*. 1834

53.   Beer, P.D.; Gale, P. A . ; Chen, G. Z. ;*Adv.Phys.Org.Chem*. 1998,31,1